Investigation of Rheological and Filtration Characteristics of NiO Nanoparticles Water-Based Drilling Fluid for HPHT Drilling

By:

Alinur Muratov

Aigerim Ismagul

Thesis supervisor:

Dr. Ali Shafiei

A thesis submitted to the School of Mining and Geosciences of Nazarbayev University in Partial Fulfillment of the Requirements for the Degree of

Bachelor of Science in Petroleum Engineering

Nazarbayev University

15 April 2023

Acknowledgements

We would like to express our sincere gratitude to our thesis supervisor, Dr. Ali Shafiei, for providing us with this opportunity to conduct this research work, for guiding us with insightful feedbacks, and for offering crucial advice throughout the research and thesis writing process. We are incredibly grateful for the opportunity to have worked with such a dedicated person.

We also like to express our gratitude to our thesis examiner, Dr. Sonny Irawan, for his helpful feedbacks, which contributed to the improvement of quality of this dissertation.

We would like to acknowledge the financial support received from Nazarbayev University through a Collaborative Research Proposal Faculty grant project (091019CRP2103) entitled "A comprehensive study on asphaltene characterization and screening asphaltene deposition inhibitors for Kazakhstan crude oils."

Special thanks to School of Mining and Geosciences at Nazarbayev University for providing access to conduct experiments in the drilling fluids laboratory. We would like to thank Mr. Gylym Sapinov and Mr. Yernur Satay for their kind assistance in the laboratory.

Originality statement

We, Alinur Muratov and Aigerim Ismagul, hereby declare that this submission is totally our own unique work and to the best of our knowledge, doesn't include any previously published or written by other authors material, nor do they contain significant portions of materials that have been approved for the award of any other degree or diploma at Nazarbayev University or any other educational institution.

The thesis makes full mention of any contributions made to the research by other people we have collaborated with NU or abroad.

We further affirm that this thesis' intellectual content is entirely our own, with the exception of any instances in which others assisted with the project's conception, design, use of language, style, and presentation.

Signed on **22.04.2023**

_____

Nomenclature

API	=	American Petroleum Institute
CM	=	custom-made
CNT	=	carbon nano tube
EOR	=	enhanced oil recovery
FLC	=	fluid loss control
GG	=	guar gum
HEC	=	hydroxy ethyl cellulose
HPAM	=	hydrolyzed polyacrylamide
HPHT	=	high pressure high temperature
LCM	=	lost circulation material
MWCNT	=	multi-walled carbon nano tube
NF	=	nanofluid
NP	=	nanoparticle
OBM	=	oil-based mud
PAC	=	polyanionic cellulose
PAM	=	polyacrylamide
PEG	=	polyethylene glycol
PHPA	=	partially hydrolyzed polyacrylamide
PNC	=	polymer nanocomposite
POCNT	=	polyethylene glycol
PV	=	plastic viscosity
ROP	=	rate of penetration
SEM	=	scanning electron microscope
SWCTs/PVP	=	synthesized single-walled carbon nanotubes/polyvinylpyrrolidone
WBM	=	water-based mud
XG	=	xanthan gum
YP	=	yield point
K	=	dimensionless consistency index, no units
N	=	index representing behavior of shear-thinning fluid flow
γ	=	shear rate, sec^{-1}
μ_a	=	apparent viscosity, Pa.s
μ_p	=	plastic viscosity, cP
τ	=	shear stress, Pa
τ_o	=	yield point, Pa

Abstract

The demand for drilling deeper wellbores to extract energy resources from deep reservoirs is growing rapidly. Drilling in formations where high temperatures and pressures are encountered is a challenging task. One important aspect of this challenge is to develop drilling fluids, which can function well in such harsh conditions. Use of nanoparticles (NPs) in various areas in petroleum engineering research has gained popularity in recent years. This is partly because of their favorable properties such as strong heat conductivity, large surface area that can significantly improve characteristics of the drilling fluid. The key benefits of using NPs in drilling fluids include a decrease in formation damage, improved heat transmission and lubrication, better control over fluid loss, and enhanced rheological properties. The main objective of this research work was to investigate the effect of using NiO NPs on rheological and fluid filtration characteristics of a water based drilling fluid prepared with this NPs under a wide range of pressure and temperature. NiO NPs were selected because they have already exhibited excellent results in EOR and asphaltene adsorption tests. The NiO NPs were characterization by using transmission electron microscope (TEM) and scanning electron microscopy (SEM). The rheological properties of the drilling fluid samples containing 0, 0.25, 0.5, and 1 wt.% of NiO NPs were measured at temperatures ranging from 25°C to 100°C. Regarding the filtration properties, the drilling fluid samples containing 0, 0.25, 0.5, and 1 wt.% of NiO NPs were tested at 130°C and 500 psi differential pressure. The results obtained from this research work showed that, the filtrate volume and filter cake thickness were lower in the test samples with NiO NPs than in the control sample. The SEM analyses of filter cake demonstrated positive effect of NiO NPs on morphology. The Herschel-Bulkley model fitted best to the experimental shear stress and shear rate data for the smart drilling fluid. The optimum concentration of NiO NPs for both rheological and rheological properties was found to be 0.25 wt%. Overall, adding NiO NPs to a water based drilling fluid enhanced its properties for HPHT conditions.

Keywords: Nanoparticles, drilling fluid, fluid loss, shear rate, yield stress, apparent viscosity, plastic viscosity.

Table of Contents

Table of Figures

List of Tables

1 Introduction

In this chapter, after providing a brief background on the need for drilling deeper in sedimentary basins and therefore the need for drilling fluids for HPHT conditions, the problem statement, research objectives, methodology, and structure of the dissertation are presented.

1.1 Background

Demand for natural gas and oil are increasing with demand for affordable energy. Consequently, more advanced and innovative technologies are being implemented for producing natural resources that were not attainable earlier. Main goal of modern additives for drilling fluid is to sustain efficiency under high pressure and high temperature for drilling deep wells. By using modern technologies, it would be possible to drill wells far deeper than earlier and produce from new reservoirs. Designing drilling mud for during deep drilling operations requires an in-depth knowledge of the important features of drilling fluid. The drilling fluid should perform several vital functions, including removing rock fragments from bottom of a well, transporting cuttings to the surface, lubricating and cooling drill bits, creating filter cake to close pores of rock formation and providing sufficient hydrostatic pressure for stable drilling (Cheraghian, 2021). Technological, financial, and environmental challenges should be considered before choosing candidates of additives for designing drilling fluids. Due to their reduced cost and environmentally friendly components, water-based fluids are the most frequently used. However, the high-pressure/high-temperature (HP/HT) conditions found in very deep wells cause WBMs to deteriorate, creating challenges for planning and conducting deep drilling operations. That is why there is a critical need to enhance rheological characteristics of drilling fluids and expand the range of downhole environments in which they can be used (Vryzas et al., 2016). Aside from rheological properties, filtrate loss properties of a drilling mud should be considered for ensuring successful drilling operation. Filtrate losses into the formation are caused due to the difference between the hydrostatic pressure produced by the drilling mud and the pressure exerted by fluids in the rock formation during drilling (Hoberock & Bratcher, 1998). In fact, the primary source of capital expenses during drilling operations is drilling fluid loss into formations. A conventional method for mitigating fluid loss is the addition of Poly Anionic Cellulose (PAC) (P. Yang et al., 2015). However, such conventional additives are not able to block nanopore throats of the wellbore (Mao

et al., 2015). Therefore, it is important to focus on development of smart drilling muds with modern additives like nanoparticles.

The effects of various additives on drilling fluid properties were investigated in past studies that aimed to improve its rheological properties and decrease filtrate invasion. Multiple investigations have been done to develop innovative drilling fluids that primarily use nanoparticles as additives. A particle can be described as a nanoparticle (NP) when at least one of its dimensions is between 1 and 100 nm (Mahmoud et al., 2018). Recent advancements in nanomaterials technology indicate that some researchers have extensively employed and analyzed applications of NPs in oil and gas sector. Applications of smart fluids for well drilling have mostly concentrated on dispersing nanoparticles in base drilling fluids to improve drilling fluid qualities (Mao et al., 2015; Saffari et al., 2018; Zhao et al., 2013). Results of past experiments and analyses demonstrated that nanoparticles might be utilized as appropriate additives to enhance the characteristics of drilling fluid under HP/HT condition. The total cost of drilling fluids can be reduced using nanoparticles that lower the chemical and solid content. The reason for this is that nanoparticles have a unique property called a high surface-to-volume ratio that allows them to seal boreholes in wells with less drilling fluid than other materials (Cheraghian, 2021). Nanoparticles are suitable materials for performing this function since they must be smaller in size than the pore throat in order to effectively plug holes in a borehole. Nanoparticles can improve wellbore stability even under HP/HT conditions because of their ability to plug nano porous formations, increasing their mechanical strength (Pourkhalil & Nakhaee, 2019; Xionghu et al., 2022). Moreover, due to their extraordinarily thin and fine size, nanomaterials can significantly reduce the coefficient of friction between drilling pipes and side holes (Cheraghian, 2021). Another advanced property of nanoparticles is their capacity for heat conductivity. Compared to conventional mud, certain nanoparticles can increase drilling fluid's heat transfer efficiency by more than 20% (Mao et al., 2015; Nguyen et al., 2012; S. Singh & Ahmed, 2010).

One of the main advantages of nanoparticles over conventional additives for decreasing filtrate loss is that nanoparticles are more environmentally friendly (Amanullah & Yu, 2005). Numerous types of NPs, including graphene (Perumalsamy et al., 2021), carbon nanotubes (Kazemi-Beydokhti & Hajiabadi, 2018), cellulose NPs, silica NPs (Hamad et al., 2019), iron oxide (Vipulanandan et al., 2015) and zinc oxide (Albajalan & Haias, 2021) have been studied in terms to their effect for minimizing filtrate loss. Each type of nanoparticle has properties like size, surface

area, surface energy, shape, chemical composition, surface roughness, and crystal structure (Vryzas & Kelessidis, 2017). Regarding the effectiveness of NPs, it was proved that they could reduce filtrate losses more than conventional additives (Ragab & Noah, 2014).

1.2 Problem statement

One of the most costly activities in the process of well development is drilling. Expenses due to filtrate invasion and formation damage can be prevented by using conventional additives for regulating filtration and rheological characteristics like poly anionic cellulose (PAC) and polyacrylamide (PAM). The problem is that conventional cannot withstand high pressure/high temperature conditions. In contrast, NPs can control rheological and filtration properties of a mud even under HPHT conditions. Using nanoparticles minimizes a number of additives, a size of a mud cake and a volume of filtrate loss (Edalatfar et al., 2021). Particularly, nanoparticles can prevent differential pressure sticking issues and also have the potential to enhance ROP (Rate of Penetration), which will lower drilling expenses (Vryzas et al., 2015). This way nanoparticles can enable drilling at high pressure/ high temperature conditions, while keeping sufficient wellbore stability. However, no research had been done about effect of NiO NPs on rheological and fluid loss properties. On top of that, laboratory experiments are necessary for finding out values of optimum concentrations.

1.3 Research objectives

The objective of this capstone project is using NiO NPs to develop a smart mud that have controllable rheological and fluid loss properties under conditions of extreme heat and pressure. The following list includes the capstone's primary research goals:

- To investigate rheological properties of the drilling fluid samples containing 0, 0.25, 0.5, and 1.0 wt.% of NiO NPs at temperatures ranging 25-100°C
- To determine the filtration properties of the drilling fluids and to investigate filter cake morphology containing 0, 0.25, 0.5, and 1.0 wt.% of NiO NPs at 130°C and 500 psi differential pressure
- To find the optimum concentration of the NiO NPs for improving rheological and filtration properties of the drilling fluid for HPHT conditions

This study might be beneficial for deep drilling operations, where conventional additives are not as efficient as nanoparticles due to high pressure/high temperature.

1.4 Relevance to the industry

The current challenge faced in petroleum industry is a development of a smart drilling mud that can withstand extreme downhole conditions such as temperature over 350°F and pressure over 10,000 psi (Aftab et al., 2017). Over time, numerous different types of nanoparticles have been explored to find out the most effective ones for mixing with drilling fluids. According to past studies, nanoparticles have a great potential for creating innovative drilling fluid. Another issue that has been addressed by utilizing nanoparticles as drilling fluid additives is borehole stability. Moreover, aside from enhancing the performance of drilling mud, nanoparticles have low cost which makes them economically favorable implementation (Abdo & Haneef, 2012). Additionally, drilling fluid with nanoparticle additives in challenging formations results in improving oil recovery (Abdo & Haneef, 2013). This can lead to higher oil production and more revenue which outweighs the cost spend on the nanoparticles and cost of non-productive time (Al-Yasiri & Al-Sallami, 2015). Nanoparticles can lower the overall cost of drilling fluids by reducing chemical and material content. Nanoparticles could lessen environmental risk and relieve ecological risk issues of drilling fluid during the many phases to generate and duplicate the drilling process (Chang et al., 2019). Past studies have shown environmentally friendly nanoparticles have the ability to decrease the adverse impacts of several toxic and heavy metals like Pb, Cu, As, Cd, Cr and Hg (Felix et al., 2018; X. Yang et al., 2017). The implementation of nanoparticles in drilling mud can be justified considering all of their economic and ecological benefits. Nanoparticles are important novelty in petroleum industry which can develop drilling fluid modifications. Thus, it is vital to pay attention to the nanoparticles that were not tested in the laboratory with drilling fluids.

1.5 Research methodology

In this study, we aim to develop a NiO nanoparticle-based drilling mud that can tolerate HPHT conditions. Our methodology consists of several key experiments including drilling fluid preparation, nanoparticle characterization, and testing the filtration and rheological properties of the smart drilling mud. Initially, WBM is prepared following the API RP13I standard. The nanoparticles are characterized using scanning electron microscopy (SEM) and transmission

electron microscopy (TEM) to determine their size and morphology. The effects of three different NiO nanoparticle concentrations on the drilling mud are evaluated. The filtration properties of the smart drilling fluid are tested using a HP/HT filter press. The filter cakes are then characterized by measuring their thickness using a caliper and analyzing their morphology using SEM images. The rheological characteristics of the drilling mud are analyzed using a rheometer, and the resulting data are fitted to the Herschel-Bulkley model.

1.6 Thesis structure

This capstone project report is divided into five chapters. In introduction (Chapter 1) a brief background is provided highlighting significance of the topic then, the problem statement, research objectives, methodology, and structure of the dissertation are presented. Chapter two contains the literature review which, consists of two parts covering previous studies about implementation of NPs for designing drilling fluids: effect of adding NPs on rheological parameters and fluid loss characteristics. The research methodology is presented in Chapter 3 in details. The procedures for NPs preparation and characterization are described and then the methods for preparation of standard water-based-mud, measurement of rheological, and fluid loss properties under different temperature and NP concentrations are described. The results and discussion makes up the Chapter 4 where the results obtained from this research work on fluid loss measurements and rheological properties are presented and discussed. A discussion of the optimum concentration point is also included. The report ends some conclusions and recommendations for future research.

2 Literature review

2.1 Rheological and filtration properties

After the mud has traveled repeatedly in and out of an HPHT well, these rheological characteristics do not always remain consistent (Agwu et al., 2021). The plastic viscosity, apparent viscosity and yield point are the main rheological characteristics of mud that can be affected by HPHT conditions.

Plastic viscosity (PV) – a parameter from Bingham model that describes the viscosity of a mud when extrapolated to infinite shear rate (SLB, 2023c). A low value of PV means that the mud has low viscosity and drilling can be done quickly, whereas a high value of PV means mud has a viscous base fluid and too many colloidal particles (SLB, 2023c).

Apparent viscosity (AV) is a measure of the resistance to flow of a fluid under the influence of an applied shear stress (SLB, 2023b). It is a dynamic viscosity value that is determined at a given shear rate or RPM. Apparent viscosity is often used to describe the flow behavior of drilling fluids, and it can vary depending on the shear rate applied to the fluid. A higher apparent viscosity indicates a higher resistance to flow, while a lower apparent viscosity indicates a lower resistance to flow.

Yield point (YP) - a parameter from Bingham model that describes extrapolating the yield stress to a zero-shear rate (SLB, 2023d). YP is used to assess the ability of a mud to transport cuttings (SLB, 2023d). A fluid with a high YP is non-Newtonian and will carry cuts more effectively than one with a lower YP but comparable density (SLB, 2023d).

Filtrate penetrates the area of the near-wellbore formation through the filter cake formed by the solid particles with one-third of pore size in drilling fluids (Al-Shargabi et al., 2022). Filtration properties can be quantified by using two parameters: fluid loss and spurt loss.

Fluid loss - leaks into the rock formation caused by solid particles from drilling fluids (SLB, 2023a). For controlling filtrate loss, following factors should be taken into account: fluid loss control (FLC) additive concentration, suspended solid size and type, drilling fluid content and system thermal stability (M. Ali et al., 2020a). Spurt Loss - the volume of filtrate that is collected before the filter cake has a chance to form (OFITE, 2015). It is measured in millimeters.

2.2 Conventional additives and their limitations

Polymers are examples of conventional additives for improving properties of drilling fluids. Effective viscosifying agents include synthetic polymers that limit fluid loss volume, such as acrylamide (AM), polyacrylamide (PAM), hydrolyzed polyacrylamide (HPAM), and partially hydrolyzed polyacrylamide (PHPA) (Wang et al., 2022). Natural polymers such as guar gum, xanthan gum, and hydroxy ethyl cellulose are frequently used to improve the rheological properties of drilling fluid and raise the yield point (Xie & Liu, 2017). However, polymers become less effective during harsh conditions. Numerous field investigations have shown that the behavior of polymers under extreme temperature and pressure conditions is neither stable nor appropriate to carry out some operational tasks that are essential in drilling operations (Sepehri et al., 2018). The poor heat conductivity and transfer qualities of polymeric additives are a major cause of thermal instability (Zhong et al., 2020). Without stability polymers are not able to provide the required viscosity for drilling operations.

The advanced technologies for deep drilling operations are in high demand due to the complicated conditions such as high temperature/pressure in unconventional reservoirs. The conventional polymeric additives cannot sustain extreme HP/HT conditions, which may lead undesired results during drilling operations (Sadeghalvaad & Sabbaghi, 2015). The integration of nanoparticles into conventionally used surfactant-based and polymeric fluids can facilitate enhancement of filtration properties and lead to the formation of stable filter cake (Fakoya & Shah, 2014). Indeed, NPs are less susceptible to deterioration when operating at high pressure and temperature (HPHT). Nanoparticles have a great potential for implementation in such environments due to their great thermal conductivity and ability to tolerate HP/HT conditions (Amanullah et al., 2009). Thermal effects are main causes for degradation of conventional additives, such as synthetic polymers (Davoodi et al., 2018). While some drilling fluids may initially withstand static HPHT conditions, with time, their characteristics may deteriorate, producing changes in drilling fluid density and filtrate volume (Zhong et al., 2019). Indeed, flocculation of clays and gelation can take place, when water-based drilling fluid is affected by extreme temperature for a long time. (M. Ali et al., 2020b). That is why novel additives such as nanoparticles and nanocomposites are being tested for designing drilling fluid that has stable rheological and filtration properties at HPHT environment.

Producing a polymer nanocomposite (PNC) involves either entrapping the polymer in the NP or impregnating the NP in the polymer (Sun et al., 2017). Studies discovered that PNC materials can be utilized for adjusting filtration properties (Ikram et al., 2020).

2.3 Types of nanoparticles

Figure 2-1 demonstrates investigated nanoparticles for improving drilling fluid filtration characteristics. Metal nanoparticles, ceramic nanoparticles, polymeric nanoparticles, and carbon-based nanoparticles are the types of nanoparticles utilized in drilling fluids (Cheraghian, 2021).

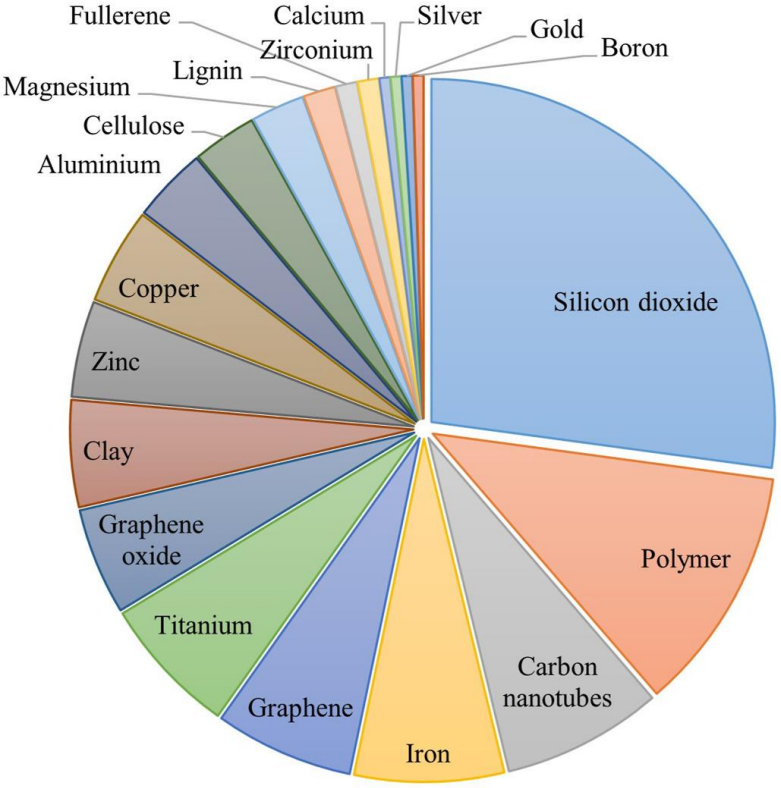

Figure 2-1. Distribution of researched nanoparticles that affect filtration properties of drilling fluids (Ibrahim et al., 2022)

Metal NPs can be synthesized via chemical, photochemical, or electrochemical methods (Cheraghian, 2021). Core of a metal NPs consists of inorganic metal or metal oxide (Al-Shargabi et al., 2022). The thermal conductivities and rheologic characteristics of water-based drilling fluids can be improved by transition metal NPs like Fe, Cu, Ag and Zr (Oseh et al., 2023).

The ceramic NPs include phosphates, carbonates of metals and oxides, and the majority of ceramics consist of silica and alumina (Sajid & Płotka-Wasylka, 2020). The ceramic nanoparticles

composed of solid core and created by heat and/or pressure application (Sajid & Płotka-Wasylka, 2020). The nanoclays are other category of ceramic nanophase which include titanium dioxide, and porous silica (Singh et al., 2016). The structure of nanoclays consist of thin layers of few nanometers and its length ranges between few hundred to few thousand nanometers (D. Singh et al., 2016).

The polymeric NPs are colloidal particles with the size ranging from 10 nm to 1 μm, that can be obtained from polymers which are environmentally friendly, biodegradable, and soluble in water (El-Masry et al., 2023; Sajid & Płotka-Wasylka, 2020). The polymeric nanoparticles can be prepared by two methods based on monomers polymerization and preformed polymers (Crucho & Barros, 2017). Polymers used during HPHT oil and gas drilling should be cost-effective, thermally stabile at downhole temperatures, soluble in base fluids, safe and environmentally friendly (Gautam et al., 2022).

Carbon-based structures are widely used in the petroleum industry, starting from diamond bits and ending with nanoparticles for enhancing properties in drilling and EOR processes. Examples of carbon based NPs are multi-walled carbon nano tubes (MWCNTs), graphene NPs and carbon black NPs (Hajiabadi et al., 2020). In contrast to other forms of nanoparticles, carbon nanoparticles are special because they have different shapes like nanoplate and nanofiber(Ibrahim et al., 2022).

2.4 Mechanism of nanoparticles for improving rheologic properties

Developing a drilling fluid that has minimal differences in its rheology profile from surface to downhole conditions is a challenging task (Bageri et al., 2019). The composition, kind, or size concentration of nanoparticles in drilling fluids can be changed based on desired drilling conditions and rheologic properties (Agwu et al., 2021). Numerous researchers proved that NPs can improve rheology of drilling fluids (Cheraghian, 2021). Figure 2-2 shows that negative charge particles of ZnTiO3 NPs can interact with the edge of bentonite, modifying the inter-particle forces (Edalatfar et al., 2021). This example shows how addition of NPs increases of attraction forces of particles in a drilling fluid, increasing rheologic properties.

Due to high value of surface area per volume, nanoparticles interact more actively with the particles inside drilling fluid, making the value of plastic viscosity larger (Das & Dutta, 2019). The

value of an YP increases as the solid additive particle sizes are reduced and attraction forces are increased (Maiti et al., 2019).

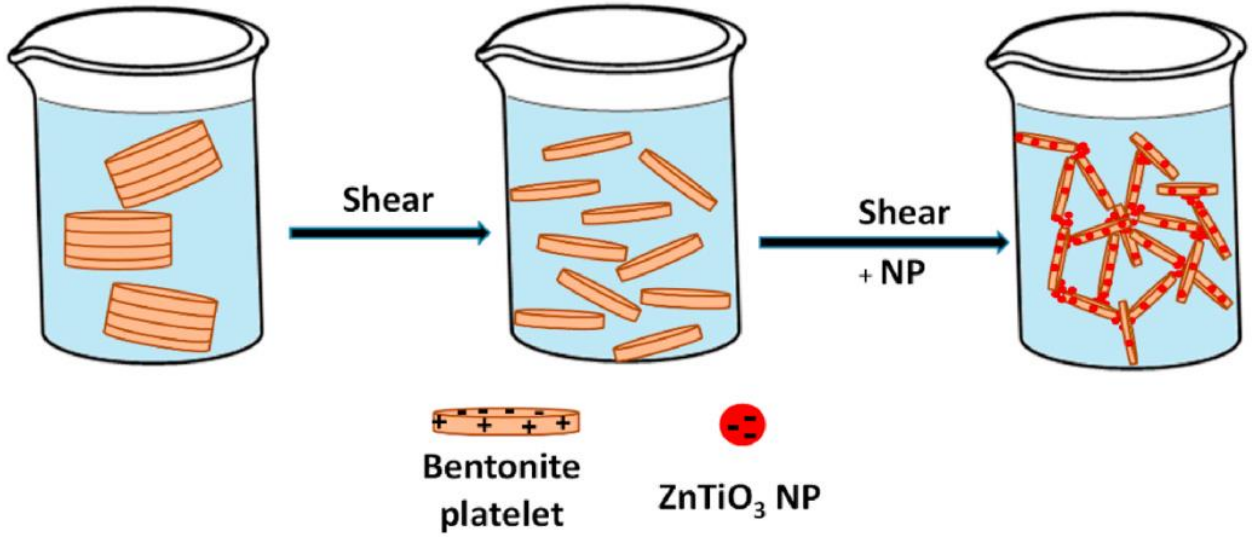

Figure 2-2. Addition of $ZnTiO_3$ into water-based drilling fluid (Edalatfar et al., 2021).

2.5 Mechanism of nanoparticles for reducing filtration loss

The volume of a fluid loss and thickness of a mud cake are key parameters in identifying and measuring the filtration loss. The control of filtration by nanoparticles is realized by changing the linkage process and filling the spaces occurred due to bentonite particles placement meaning that the occupation of pathways between particles leads to filtration reduction (Salih & Bilgesu, 2017). The study by Salih and Bilgesu (2017) showed that nanosilica is able to seal the narrow space caused by bonding between the flocculated bentonite particles due to its smaller size compared to other anionic nanoparticles (nanotitanium, nanoaluminium).

Figure 2-3(a) shows how addition of big particles of lost circulation material (LCM) block the invasion into formation. This seal gets even more effective for reducing filtration when smaller nanoparticles fill the gaps between LCM as shown in Figure 2-3(b). That is how nanoparticles can solve the problem of fluid loss by forming impermeable mud cake.

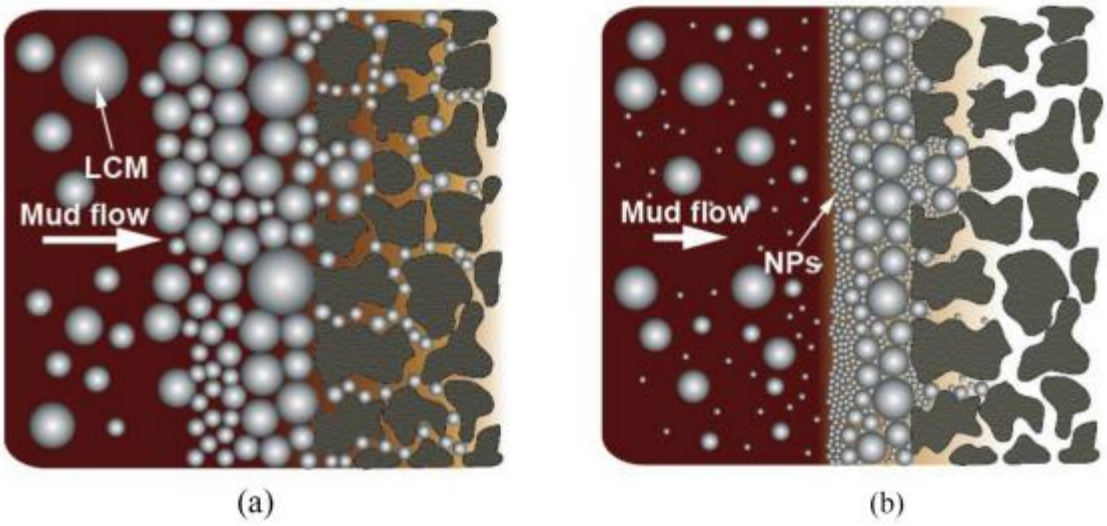

Figure 2-3. Reduction of filtration loss by using (a) conventional LCM and (b) nanoparticles (Contreras et al., 2014).

2.6 Effect of nanoparticles on rheological properties

Rheological characteristics of drilling are very important for planning successful drilling work. The success of a drilling operation can be considerably impacted by the effect of temperature and pressure on rheological characteristics. In addition, knowing the rheology of drilling fluid accurately is essential for accurate predictions of frictional losses (Gavignet & Wick, 1987). Previous studies investigating effect of nanoparticles on rheologic properties presented here:

2.6.1 *Fe_3O_4 nanoparticles*

The addition of NPs can considerably affect the shear stress behavior of drilling fluid. For example, adding 0.5 wt% Fe_3O_4 nanoparticles in a water-based mud resulted in an upward shift of the rheogram roughly by +10% (Vryzas et al., 2016). This effect can be explained by considering the effect of bentonite particle gelation, primarily controlled by electrical forces, which appears to be lessened by adding NPs (Van Olphen, 1964). Particle size and surface area of nanoparticles were 6-8 nm and 100-260 m^2/g.

2.6.2 *$ZnTiO_3$ nanoparticles*

Mixing $ZnTiO_3$ nanoparticles with water-based drilling fluid enhances shear thinning behavior and increases the viscosity (Edalatfar et al., 2021). This behavior can be explained by looking at Figure 2-2. The average size of nanoparticles was 40–160 nm.

2.6.3 *Nanosilica*

Addition of nanosilica into drilling mud can improve its rheological characteristics. For instance, when 1.0 ppb of nanosilica is added, the PV of each sample of WBM basic mud decreased from 28 to 15 cp, 31 to 21 cp, 22 to 18 cp, and 22 cp to 15 cp at temperatures 77°F, 150°F, 250°F, and 300 °F, respectively (Katende et al., 2019). Reduction of viscosity is partially achieved through stabilized dispersion. Stabilized dispersion of nanoparticles is ensured by charging nanosilica's surfaces and creating self-repulsions, as shown in Figure 2-4. Stabilization of nanoparticles is an important step because it prevents agglomeration that can lead to precipitation. The particle size and surface area of nanoparticles were 14 nm and 202 m^2/g.

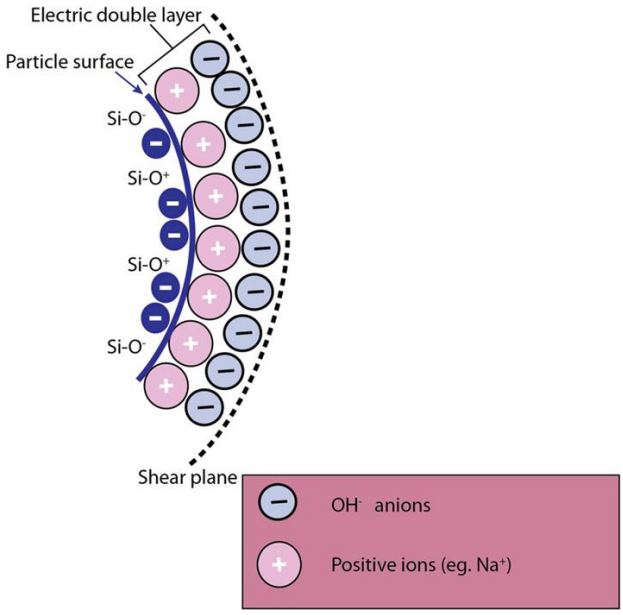

Figure 2-4. Self-repulsion as a result of charging the surface of nanosilica (Katende et al., 2019).

2.6.4 *Nanotubes*

Figure 2-5 shows the effect of adding carbon nanotubes into oil-based mud. Based on the trend of Figure 2-5, it can be stated that the concentration of nanoparticles is directly proportional to the rheological properties of mud.

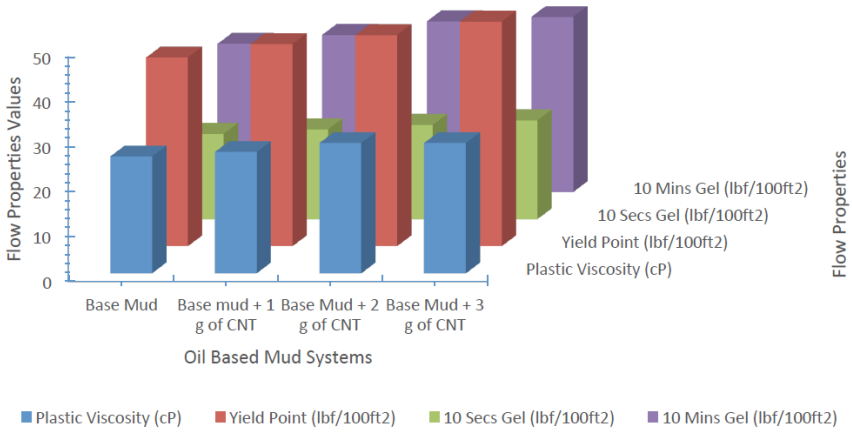

Figure 2-5. Effect of Carbon Nanotubes on the rheological properties *(Okoro et al., 2021)*

2.6.5 *SiO_2 and ZnO nanoparticles*

Rheological properties of WBM can be enhanced by adding SiO_2 and ZnO nanoparticles. By conducting experiments, it was found that plastic viscosity decreased by 8% and 23 % when the concentration of SiO_2 and ZnO nanoparticles increased from 0 to 1 wt. % (Albajalan & Haias, 2021). The addition of nanoparticles minimized friction forces between particles, which decreased plastic viscosity (Albajalan & Haias, 2021). On top of that, in the same study addition of SiO_2 and ZnO nanoparticles resulted in a yield point decrease of 4.8% and 4.5% (Albajalan & Haias, 2021). The yield point was reduced because added nanoparticles increased the distance between clay particles (Albajalan & Haias, 2021). SiO_2 had a particle size of 15-20 nm and a surface area of 180–270 m^2/g, whereas ZnO had a particle size of 10-320 nm and a surface area of 88.89 m^2/g.

2.6.6 *TiO_2, SiO_2, and ZnO nanoparticles*

Another study tested the effect of TiO_2, SiO_2, and ZnO NPs on rheological properties. Bayat and Shams (2019) found that ZnO is the best choice for decreasing plastic viscosity, whereas TiO_2 decreased yield point. Regarding SiO_2, it increased yield points and was the best choice for increasing gel strength (Bayat & Shams, 2019a). All nanoparticles had a particle size of 20 nm. What about the surface area, 50-100 m^2/g for TiO_2, 67 m^2/g for ZnO, and 160 m^2/g for SiO_2.

2.6.7 *Al_2O3, SiO_2, and TiO_2 nanoparticles*

Misbah et al. (2022) tested how Al_2O_3, SiO_2, and TiO_2 nanoparticles affect the rheology of water-based drilling mud. Figure 2-6 shows how shear stress was reduced by 12–76% after adding

nanoparticles. Moreover, TiO_2 nanofluids dramatically decreased viscosity by 43-77% at low volume fractions of 0.05%, and Al_2O_3 significantly decreased viscosity by 22-49% at a volume fraction of 1.0%. (Misbah et al., 2022). TiO_2 had a particle size of 18 nm, Al_2O_3 had a particle size of 27-43 nm, and SiO_2 had a particle size of 18-20 nm. The surface area of TiO_2 was 200–240, whereas for Al_2O_3 it was 35 m^2/g.

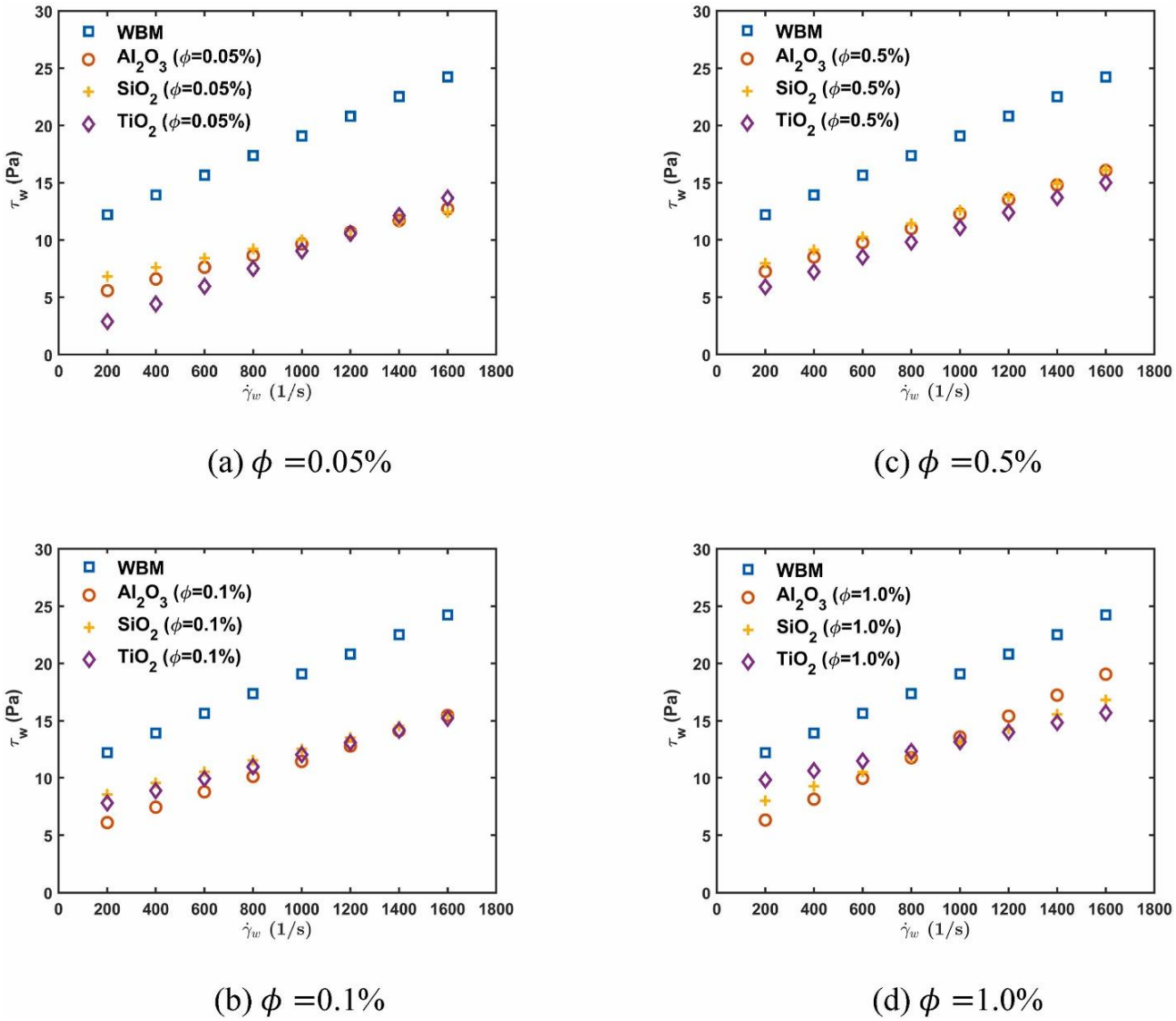

Figure 2-6. Shear stress effect of nanoparticles (Misbah et al., 2022).

2.7 Effect of nanoparticles on fluid loss properties

Fluid losses occur during drilling operations when the drilling fluid enters the porous media. The porous media's porosity and permeability significantly impact the fluid losses. Drilling fluid loss into the formation can lead to an irreversible change of density, which could cause borehole instability. The invasion of fluid into the porous formation is hazardous, as this fluid can obstruct the hydrocarbon flow channels, lowering the reservoir's productivity and inducing formation collapse (Kosynkin et al., 2012). Therefore, preventing fluid loss should be a crucial concern during downhole operations. One of the critical features of nanoparticle application is that NPs can control fluid loss. The nanoparticle-based fluid loss control additives are able to form filter cakes that would cover the wellbore and slow the fluid loss through porous formation (Kosynkin et al., 2012). This literature review section will review studies about nanoparticle-based drilling fluids and their ability to enhance fluid loss control during drilling operations.

2.7.1 *Nanoclays*

It is hypothesized that the surfaces of bentonite clay have a net negative charge and are covered with clouds of cations, because of the electron shortage caused by isomorphic substitution in their unit layer (Zhao et al., 2013). As a result, functionalized and charged nanoparticles can change the rheological characteristics of drilling fluids by exerting attracting and repulsive electrostatic forces. Zhao et al. (2013) stated that drilling fluid systems may experience an increase or decrease in the amount of fluid loss due to electrostatic contact. Such complications make the smart drilling mud research area attractive for researchers to overcome challenges that may arise during petroleum drilling operations.

The study by Vipulanandan and Mohammed (2018) examined the fluid loss of drilling fluids made of bentonite modified with nanoclay at various temperatures. In order to forecast fluid loss over the short- and long-term with respect to time and to compare it to the API fluid loss model, the Vipulanandan fluid loss model was proposed (Vipulanandan & Mohammed, 2018). The Vipulanandan fluid loss model was successful in predicting the short- and long-term fluid loss with time, nanoclay concentration, and temperature since it had a lower root mean square error than the API fluid loss model.

2.7.2 *Magnetic nanoparticles*

Vryzas et al. (2018) studied the thermal stability of water-based mud when magnetic NPs were added, and suggested managing drilling fluid characteristics including rheology and fluid loss, which can be done at temperatures of roughly 121°C. On the basis of this study, the use of MR fluids in drilling operations for HP/HT conditions may be taken into consideration. Another research study by Vryzas (2016) focused on a method for applying new magnetite nanoparticles that would improve the qualities of smart drilling fluid under HP/HT circumstances. The inclusion of 0.5 wt% CM Fe3O4 NPs resulted in a 40% reduction in HP/HT fluid loss relative to the base fluid before aging and an even greater reduction of 43% after thermal aging.

2.7.3 *Metal oxide NPs*

The research by Bayat et al. (2018) revealed that TiO_2 based nanoparticles has a great potential in reducing the fluid loss compared to the Al_2O_3, CuO and SiO_2. Moreover, TiO_2 nanoparticles make smooth and stable filter-cake as it provides better particle compression (Bayat et al., 2018). Another study showed that TiO_2 NPs and ZnO NPs are the best fluid loss control agents at temperature of 25°C and 50°C, respectively (Bayat & Shams, 2019b).

2.7.4 *Carbon based nanoparticles*

Among various types of additives for the drilling muds, carbon-based nanoparticles are found to be more efficient because of their wide availability, ease of preparation, economic cost, and remarkable mechanical and thermal properties (An et al., 2018; Kazemi-Beydokhti & Hajiabadi, 2018).

Carbon nanotubes (CNTs) are revealed to be effective in enhancing drilling mud characteristics among different carbon-based nanoparticles (Rana et al., 2020). According to the study by Ismail et al. (2016), a multi-walled carbon nanotube (MWCT) is the most effective material to prevent filtrate loss compared to nanosilica and glass beads. This study explains the effectiveness of multi-walled carbon nanotubes by pointing to their high surface area and nanotube structure. Another study investigated the sample of the mixture of water-based drilling mud and carbon nanotubes that showed filtrate reduction, and subsequent discovery revealed its sustainability under HPHT conditions (Fazelabdolabadi et al., 2015).

One more type of carbon-based nanoparticle is graphene oxide, which sustains shape morphology and allows required pore plugging during filter cake development (Kosynkin et al., 2012). The study by Kosynkin et al. (2012) obtained the graphite oxide from natural graphite

flaskes that was able to penetrate through pores by creating starfish shapes much smaller than the original shape of the nanoparticle. During this research, the API filtration test showed that applying graphene oxide as an additive can reduce fluid loss by leaving a filter cake with a thickness of 280 μm compared to the 20 μm filter cake of standard polymer-based additives conventionally used in the oil and gas sector (Kosynkin et al., 2012).

2.7.5 *Ceramic NPs*

The study by Srivatsa and Ziaja (2012) investigated colloidal silica NPs as fluid loss additives. API filter press tests on samples with increasing concentrations of nanoparticles by 30% revealed that fluid loss decreased by 2 mL (Srivatsa & Ziaja, 2012). However, the performance of the fluid may be hampered rather than enhanced by the aggregation of NPs in the polymer fluid, which might lead to the development of an inefficient filter cake (Srivatsa & Ziaja, 2012).

2.7.6 *Nanocomposites*

The different types of nanomaterials can exhibit a wide range of functions, and their influence on drilling fluid properties differs significantly. One type may enhance one property of the nanomaterial but may not influence other properties (Muhsan et al., 2017; Taha et al., 2015). It is improbable to consider that adding a single nanoparticle can enhance all associated properties. The past studies faced difficulty formulating the composition of the drilling mud that would lead to adequate results for the static and flow conditions of drilling mud (Al-Yasiri & Wen, 2019). Moreover, the drilling fluids display viscous and elastic behavior, functioning as viscoelastic materials. The studies on the viscoelasticity of smart drilling fluids with nanomaterials are limited.

The study by Al-Yasiri and Wen (2019) showed that Gr-Al_2O_3 nanoparticles integrated into water-based drilling mud containing bentonite could reduce fluid loss by forming an impermeable cake. This research showed that the application of such hybrid composite could improve drilling mud properties due to the large surface-to-volume ratio and high electrical and thermal conductivities, while the presence of graphite can reduce filtrate loss because of its morphology (Al-Yasiri & Wen, 2019).

Aftab et al. (2020) synthesized ZnO using an environmentally friendly hydrothermal method; this nanocomposite mitigated a HPHT filtration loss by 30% and minimized the instability of the wellbore. The nanocomposites of carbon nanotubes with different additives can also improve fluid loss control. Rana et al. (2020) synthesized single-walled carbon nanotubes/polyvinylpyrrolidone (SWCTs/PVP) using the ultrasonic dispersion method and revealed that SWCTs/PVP-based

nanocomposite can reduce fluid loss into permeable formation. According to this study, SWCTs can be effectively dispersed in a PVP matrix by an ultrasonic approach, which creates a thick filter cake with lower permeability that blocks the fluid flow through its surface, thereby improving fluid loss control (Rana et al., 2020). Kazemi-Beydokhti and Hajiabadi (2018) showed that the composite of MWCTs and polyethylene glycol (PEG) can substantially decrease the mud cake permeability, lowering the mud filtration volume by 82% due to the modification of the mud cake structure by MWCT and wrapped by PEG.

Table 2.7-1. Summary of past research studying effect of nanoparticles on rheological and filtration properties of drilling mud

Reference	NP	Base of fluid	Size/Concentration	Surface area	Modified parameters	Conditions	Results
(Vryzas et al., 2016)	Fe_3O_4	WBM	Average diameter of 6-8 nm	100-260 m^2/g	Yield stress, viscosity, and gel strength	Fluid loss characteristics were examined under 20.7 bar and 121°C	• A linear dependence of yield stress on temperature of the produced nanofluids (NF) was identified. • The best rheological and filtration properties were achieved by adding Fe3O4 NPs at 0.5 weight percent.
(Edalatfar et al., 2021)	$ZnTiO_3$	WBM	Average size of around 40–160 nm		Viscosity, yield stress, shear rate	90◦C	• The addition of 1wt% $ZnTiO_3$ NPs reduced the volume of fluid loss by about 7.7%.
(Xuan et al., 2014)	Nanographite oxide	WBM	0.6 wt %		Plastic viscosity	100◦C 150◦C 200◦C	• Nanographite show stability up to 150 °C and decomposed at ∼180 °C.
(Katende et al., 2019)	Nanosilica nanoparticles	WBM, OBM	Average size of 14 nm Concentration variation: 0.5 ppb to 1.5 ppb	202 m^2/g	Plastic viscosity, electrical stability, yield point, shear rate, gel strength, filtration loss	From ambient temperature to 300 °F	• The use of nanosilica can effectively improve the majority of the rheological characteristics of both WBM and OBM.
(Albajalan & Haias, 2021)	SiO_2 and ZnO	WBM	15-20 nm for SiO_2 10-30 nm for ZnO Concentrations of nanoparticles ranged from 0.25 to 1 wt.%	180–270 m^2/g for SiO_2 88.89 m^2/g for ZnO	Plastic viscosity, electrical stability, gel strength	100 psi, HT	• NPs were used for minimizing the thickness of mud cake, reducing the filtration volumes, and adjusting the friction factor
(Bayat & Shams, 2019b)	SiO_2, ZnO and TiO_2	WBM	20 nm for SiO_2, ZnO and TiO_2 10-20 nm for Na_2CO_3 and Bentonite	50-100 m^2/g for TiO_2 67 m^2/g for ZnO 160 m^2/g for SiO_2 11 m^2/g for Na_2CO_3 124 m^2/g for Bentonite	Plastic viscosity, electrical stability, gel strength, filtrate loss	25 and 50 °C	• The ideal concentrations of ZnO, TiO_2, and SiO_2 NPs were discovered to be 0.05, 0.01, and 0.1 wt%, respectively. Additionally, ZnO and SiO_2 NPs showed the superior filtration loss control performances at concentrations below 0.05 wt%.
(Kazemi-Beydokhti & Hajiabadi, 2018)	Oxidized multi-walled carbon nanotube wrapped by polyethylene glycol (POCNT)	WBM	20-30 nm	>110 m^2	Viscosity, yield stress	100 psi 30 °C and 40 °C	• At various temperatures, the addition of POCNT in WBMs has been found to improve the viscosity, yield stress, and ultimately the carrying capacity of the drilling muds.
(Vipulanandan et al., 2017)	Iron oxide nanoparticles ($nanoFe_2O_3$)	WBM	30 nm The nano Fe_2O_3 contents were varied up to 1% by the weight	38 m^2/gm	Yield point, shear stress, resistivity, plastic viscosity	The temperature was varied from 25°C to 85°C	• As the bentonite and nano Fe_2O_3 contents rose, the drilling mud's electrical resistance dropped. The yield stress, shear thinning behavior, and ultimate shear stress limit of the

							drilling mud were changed by the addition of nano Fe_2O_3 up to 1%.
(Misbah et al., 2022)	Al_2O_3, SiO_2, and TiO_2 nanoparticles	WBM	18 nm for TiO_2 27-43 nm for Al_2O_3 Al_2O_3, SiO_2, and TiO_2: volume fractions of 0.05%, 0.1%, 0.5% and 1%	200-240 m^2/g for TiO_2 35 m^2/g for SiO_2	Apparent viscosity, yield stress, Darcy friction factor	Below 40 °C for nanoparticles preparation	• Al_2O_3 nanofluids have only succeeded in decreasing the Darcy friction factor by 23-50%. The average Darcy friction factor has been lowered by 40% with SiO_2 nanofluids. TiO_2 nanofluids significantly (42–76%) lowered the Darcy friction factor in the TCS.
(Ismail et al., 2016)	Multi-walled carbon nanotube (MWCNT), nanosilica, glass beads	WBM	MWCNT (21 nm), nanosilica (12 nm), GBs (90–150 μm), GBs (250–425 μm)		Plastic viscosity, yield point, gel strength	Filtrate volume was determined at API conditions (100 psi and ambient temperature)	• After 0.01 ppb concentration of nanoparticles, the PV provides the increasing trend. MWCNT and nanosilica exhibited the same trend after 0.1 ppb. MWCNT decreased the PV because it may improve volume of suspended material in the drilling fluid.
(Ao et al., 2021)	Zwitterionic silica-based hybrid nanomaterial	WBM	Spherical morphology (50−150 nm)		Apparent viscosity (AV), plastic viscosity (PV), and yield value (YP)	Temperature range of 25–600 °C.	• ZSHNM nanoparticles could fill pores and cracks among the Na-Bent particles to form a dense filter cake with high hydrophobicity and low permeability. As a result, the fluid loss of BT-WBDFs was efficiently prevented.
(Cheng et al., 2022)	Tetrameric poly (VS-St-BMA-BA) nanoparticles	WBM	Ranged from 62.17 to 96.44 nm, with a median particle size of 75.8 nm		Apparent viscosity, plastic viscosity, yield point.	High temperature of 359.5 °C	• The plugging rate of artificial mud cake and artificial core reached 48.18 and 88.75%, respectively, when the amount of poly (VS-St-BMA-BA) was added at 2.0%
(Song et al., 2016)	Cellulose Nanocrystal, Cellulose Nanofibers	WBM	3.5 g each		Filtration loss	200°F 1000 psi	• The thickness of filter cakes soon rose as additional CNPs were utilized, reaching 0.28 cm for BT10/CNC3.50 and 0.32 cm for BT10/CNF3.50.

(J. A. Ali et al., 2022)	SiO_2/KCl/ Xanthan nanocomposites	WBM			Yield point, Plastic viscosity, and gel strength Filtration properties	30 and 90 °C, 100 and 600 psi	• The plastic's viscosity, yield point, and gel strength were increased from 4 cP, 10 lb/100 ft2, and 27 lb/100 ft2 to 19 cP, 62 lb/100 ft2, and 54 lb/100 ft2, respectively
(Sajjadian et al., 2022)	ZnO, TiO_2, untreated and functionalized MWCNs	WBM	22.24 nm (U-MWCNTs,), 14.57 nm (F-MWCNT), 5.2 nm (TiO_2) 68 nm (ZnO)	60 m^2/g (U-MWCNT, F-MWCNT),	Yield stress, Plastic viscosity, and gel strength Filtration properties	500 psi 180 and 200°C	• The filtration results demonstrated that, particularly in HPHT settings, the poly (AN-co-VP)/zeolite composite with F-MWCNTs might aid to prevent the rise of filtration loss of the mud samples.
(Jia et al., 2022)	Polymer grafted silica nanocomposite	WBM	200 nm		Yield stress, Plastic viscosity, and Gel strength Filtration properties	200 °C, 230 °C and 260 °C 500 psi	• Lower plastic viscosity and greater yield point were obtained when copolymer content was 2 wt%.
(Razak Ismail et al., 2014)	MWCNT, TiO_2, Al_2O_3 and CuO	WBM, SBM	MWCNT: 0.001 g, 0.01 g, 0.1 g, 1 g of 1 wt.%		Mud weight, Yield point, Plastic viscosity, Gel strength, Filtrate loss and Filter cake thickness	250 °F and aging at 16 hours	• MWCNT (1 g): 65% filtrate loss reduction, and 30% mud cake thickness reduction. • WBM with titanium oxide: 50% fluid loss reduction, and 30% filter cake thickness reduction. • TiO_2 and CuO: decrease in plastic viscosity, yield point and gel strength.
(Al-Saba et al., 2018)	CuO, MgO and Al_2O_3	WBM	Size: 40 nm of CuO, 20 nm of MgO, 27-43 nm of Al_2O_3 Concentration: 0.5 % Vol.		Yield point, Plastic viscosity, Gel strength and Filtration properties	120°F HPHT filter press at 500 psi and 250°F	• At 120°F: improved gel strength by 218% and yield point by 368%. • The filtration characteristics are negatively affected at HPHT.
(Zhong et al., 2021)	Bentonite-hydrothermal carbon nanocomposites (BHCN)	WBM	1.0 wt% nanocomposite materials		Yield point, Plastic viscosity, Apparent Viscosity and Filtration properties	at 220 °C and 240 °C	• The filtration loss is reduced by 41% at 220 °C and 44% at 240 °C. • Improved rheological properties under ultra HPHT conditions.

(Smith et al., 2018)	SiO_2 Al_2O_3	WBM	SiO_2: 12 nm; 0.1, 0.2, 0.5, 1 wt% Al_2O_3: <50 nm; 0.1, 0.2, 0.5, 1 wt%	Al_2O_3: 40 m^2/g SiO_2: 175-225 m^2/g	Yield point, Plastic viscosity, Apparent Viscosity and Filtration properties	at 500 psi and 120°C	• At lower concentrations of SiO_2 and Al_2O_3, the filtration is decreased. • At higher concentrations of SiO_2 and Al_2O_3, the rheology parameters degraded less.
(Ahmed Mansoor et al., 2021)	Aloe-vera-based CuO nanofluid	WDF	CuO: 0.2, 0.4, 0.6 wt% Spherical shape of CuO NPs is less than 40 nm		Rheological and Filtration properties.	100 psi	• NF-WDF improves the filtration by 66%. • The rheological properties obtained stability at addition of 0.6 wt% of nanofluid.
(Fakoya & Shah, 2014)	ZnO $CaCO_3$	OBM	6 nm for ZnO 64 TO 100 nm for $CaCO_3$ 5%		Yield point, Plastic viscosity, Filtration properties	Filter press at 500 psi and 350°F Viscometer at 120°F and 500 psi	• The addition of 0.5 of modified calcium carbonate with 0.5 of the PSBR polymer: The yield point increased from 16 to 23. The fluid losses decreased from 12 to 7. • The addition 0.5 of ZnO-NPs to 0.5 PSBR polymer: The plastic viscosity increased from 22 to 31. The yield point from 16 to 26. The fluid losses decreased from 12 to 6.
(Sajjadian et al., 2020)	ZrO_2 TiO_2 FMWCNT	WBM	ZrO_2 4.46 nm TiO_2 100 nm FMWCNT 14 nm 0.5 wt%	ZrO_2 85 m^2/g TiO_2 80 - 100 m^2/g FMWCNT 220 m^2/g	Yield point, Plastic viscosity, Filtrate volume, Mud cake thickness	500 psi and 93 °C	• MWNT-TiO_2 hybrids and ZrO_2 increased the yield point, plastic viscosity and the gel strength of the drilling muds. • By using multi-wall carbon nanotubes, the yield point increased nearly from 5 at 0.057 wt% to 20% at 1 wt%.

3 Methodology

This research work is focused on investigation of rheological and filtration characteristics of NiO NPs based drilling mud that can tolerate HPHT conditions. The first step will be preparation of drilling fluid, then the nanoparticles will be characterized by SEM. The filtration properties of the nanoparticle-based drilling fluid will be tested by HP/HT filter press. The size of filter cakes will be measured by caliper and morphology of obtained filter caked will be studied by using SEM images. The rheological characteristics of drilling mud will be tested by rheometer. The following flowcharts demonstrate the steps of laboratory experiment which is going to be performed:

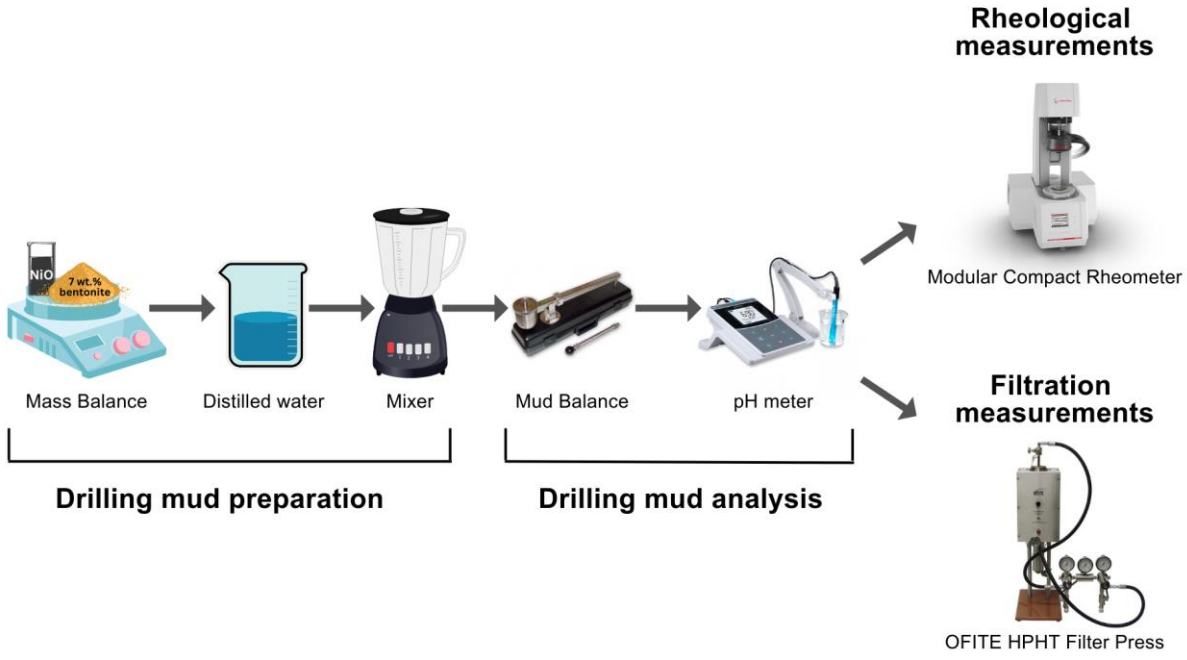

Figure 3-1. Flow chart for drilling fluid preparation.

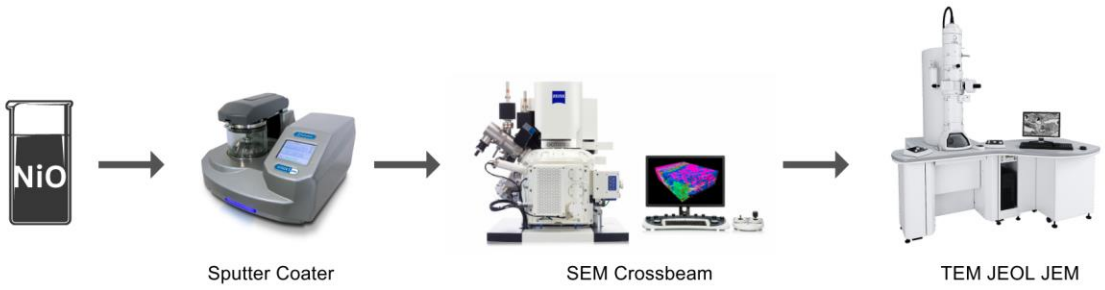

Figure 3-2. Flow chart for NiO nanoparticle characterization.

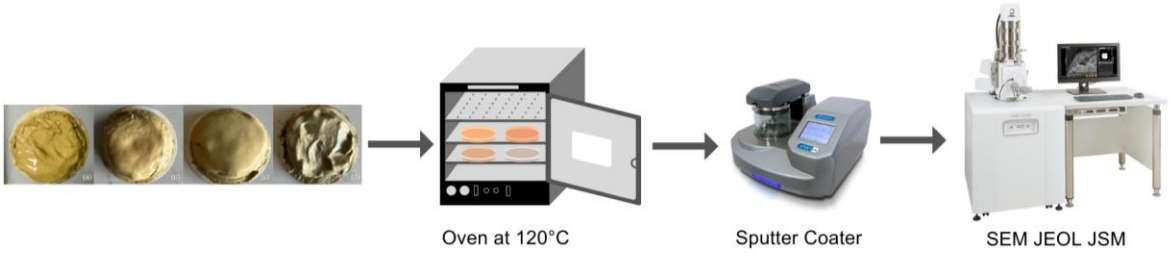

Figure 3-3. Flow chart for a filter cake characterization.

3.1 Drilling fluid preparation

Instructions from API (American Petroleum Institute) RP13I standard were used for preparing water-based mud (WBM) (API Specifications 13B-1, 2009). A standard drilling mud was chosen to eliminate the effect of other additives. The effects of three different NiO NPs concentrations were evaluated. 300 ml of distilled freshwater and bentonite with density 2.6 gm/cm^3 were mixed for 20 minutes. Mass of bentonite and nanoparticles that were used in the following experiments are given in Table 3.1-1. Initially, 22.581 g of bentonite was added to 300 ml of fresh water. This solution was mixed for 20 minutes by using Hamilton Beach mixer shown in Figure 3-4. After addition of nanoparticles into the next samples, the solution was mixed for another 20 minutes. Then, a mud balance Model 140 shown in Figure 3-5 was used for measurement of density of the drilling fluid. The density of prepared samples was equal to 8.72 ppg. A pH meter was used to measure acidity of the prepared solution. The value of the pH was in the range between 7.1-7.4.

Figure 3-4. Hamilton Beach mixer (Hamilton beach, 2023).

Table 3.1-1. Composition of drilling mud.

Mud sample	Distilled freshwater (ml)	Bentonite (g)	NiO concentration (wt. %)	NiO weight (g)	Mixing time (min)
Mud-1	300	22.581	0.000	0.000	20
Mud-2 + 0.25 wt. %		22.641	0.250	0.806	
Mud-3 + 0.5 wt. %		22.702	0.500	1.613	
Mud-4 + 1.0 wt. %		22.823	1.000	3.226	

Figure 3-5. OFI Pressurized Mud Balance.

3.2 Nanoparticle selection

NiO nanoparticle was selected for the study. NiO were provided by Nanoshel a Nanotechnology Company. According to information provided by the manufacturer in Figure 3-6, NiO nanoparticles have an average particle size of lower than 80 nm and with 99.9% purity. The color of NiO NPs is black and shape is spherical. The molecular weight of NiO is 74.69 g/mol. Additionally, SEM was used for analyzing morphology and measuring the size of the nanoparticles. Different concentrations of NiO (0.25, 0.5, 1.0 wt %) nanoparticles are used as an additive to the base mud.

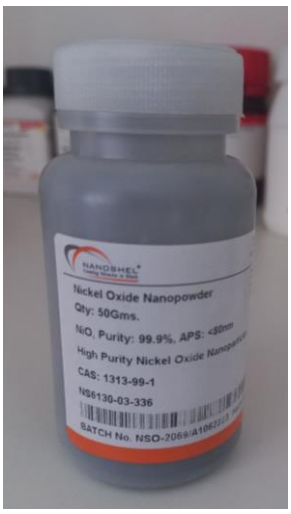

Figure 3-6. NiO Nanopowder

3.3 NiO NPs characterization by using Scanning Electron Microscope

Morphology of NiO NPs is determined by Scanning Electron Microscope (SEM) Zeiss Crossbeam 540 (Figure 3-7). The NiO NPs sample was mounted onto an SEM sample holder using conductive adhesive tape, and to improve conductivity and reduce charging effects, the samples were sputter-coated with a thin layer of gold. The SEM instrument was equipped with a field emission electron source and an energy-selective backscattered electron (EsB) detector for enhanced imaging. The accelerating voltage was set to 5 kV, depending on the desired image resolution. The working distance was adjusted to obtain optimal resolution and signal-to-noise ratio for each sample. High-resolution SEM micrographs were captured at various magnifications, ranging from 2,000x to 50,000x, to examine the NiO nanoparticles' morphology and agglomeration behavior. Images were analyzed using image processing software to quantify particle size distribution and identify any recurring patterns or structures. These findings are crucial for understanding the impact of incorporating NiO nanoparticles as an additive in drilling fluids.

Figure 3-7. Scanning Electron Microscope ZEISS Crossbeam 540.

3.4 NiO NPs characterization by using Transmission Electron Microscope

The grain size of nanoparticle is measured by Transmission Electron Microscopy (TEM) JEOL JEM - 1400 Plus shown in Figure 3-8. The TEM is operated at a voltage of 80 kV. For proper electron penetration rate, the TEM should run at a high voltage. The electron cannon, electrostatic lenses that direct electrons before and after the specimen, and a detecting device that focuses on transmitted electrons are all included in the TEM. The electrons that are transmitted through the nanoparticle are later captured by parallel detector to create a resulting image (Inkson, 2016). The TEM provided images with the resolution of 100 nm.

Figure 3-8. The Transmission Electron Microscope JEOL JEM - 1400 Plus.

3.5 HP/HT filter press

Figure 3-9 shows HP/HT filter press that was used for measuring filtration properties of the prepared drilling fluid samples. The apparatus consists of manifold block, thermostat, two nitrogen pressure regulators, a controlled pressure source, a controlled pressure source and a suitable stand. A nitrogen source was implemented to regulate the pressure values, whereas the temperature was regulated by using a heating jacket. The maximum operating temperature and pressure of HP/HT filter press are 400°F and 2000 psi, respectively. Filtration area of HTHP filter press is 22.9 cm^2, whereas the area of a standard filtration test is 45.8 cm^2 (OFITE, 2015).

Preparation and operation of filtration process were conducted by using instructions from manufacturer (OFITE, 2015). In the beginning, the equipment was assembled with applying grease to the O-rings and ensuring that all threads are clean of debris. Then, an inlet of the cell was

screwed into the cell body. Next, the O-ring was placed on valve stems. After successful inspection, the cell body was inverted, and the freshly prepared drilling-fluid samples were placed in the cell. This was followed by placing a standard ceramic filter disk with 2.5-in. diameter on top of the cell O-ring. Regarding properties of the ceramic disk, the permeability was equal to 775 mD and the average pore size was equal to 10 μm. After screwing the valve stem tightly, the cell was inverted and placed in the heating jacket. A short time later, the block from the dual Nitrogen manifold was connected to the top valve stem. The dual Nitrogen manifold's hose was then screwed into the back pressure receiver. Finally, the valve stem was opened 1⁄2 turn. A top pressure of 600 psi and bottom (back) pressure of 100 psi was applied. After waiting 1 hour for the temperature stabilization at 266°F the outlet valve stem was opened to start filtration. The liquid that passed through ceramic disk was then collected by measuring cylinder up to the valve port and carefully opening the ball valve on the back pressure receiver. The filtrate was collected at intervals of 10 sec, 1 min, 7.5 min and 30 min. A caliper was used to measure the thickness of a filter cake. The morphology of filter cakes was further examined by using SEM.

Figure 3-9. OFITE HTHP Filter Press with Threaded Cells.

3.6 Filter cake characterization by using Scanning Electron Microscope

The morphology of filter cakes' samples was analyzed by using Scanning electron microscopy (SEM) JEOL JSM-IT200 (Figure 3-10). The samples were first air-dried at room temperature for 24 hours and heated in the oven for 3 hours under 120°C to remove any residual moisture. Once dried, the samples were gently crushed into small fragments ensuring that the particle sizes remained within the range of interest. To prepare the samples for SEM analysis, the fragments were mounted onto an SEM sample holder with conductive adhesive tape to ensure proper electrical grounding during imaging. Before introducing the samples into the microscope chamber, they were sputter-coated with a thin layer of gold to enhance conductivity and reduce charging effects. The SEM instrument was equipped with a tungsten filament electron source, a low-angle backscatter detector (LA-BSD) for enhanced imaging, and an integrated Energy-Dispersive X-ray Spectroscopy (EDS) system for elemental composition analysis. The accelerating voltage was set to 15 kV, depending on the desired image resolution. The working distance was adjusted to obtain optimal resolution and signal-to-noise ratio for each sample. High-resolution SEM micrographs were captured at various magnifications, to examine the filter cake's morphology, including particle shapes and sizes, and their distribution within the sample. Images were analyzed using image processing software to quantify particle size distribution and identify any recurring patterns or structures.

The EDS system was utilized to analyze the elemental composition of the filter cake samples. Point analysis was performed on specific areas of interest, while elemental maps were acquired to determine the spatial distribution of elements within the filter cake samples. The EDS data were processed using dedicated software to identify and quantify the elemental composition of the samples. The test duration is 30 minutes for all four samples. This detailed methodology allowed for a thorough characterization of filter cake morphology, particle size distribution, and elemental composition, providing valuable insights into its structure, properties, and the impact of drilling fluid composition and formation characteristics on filter cake formation.

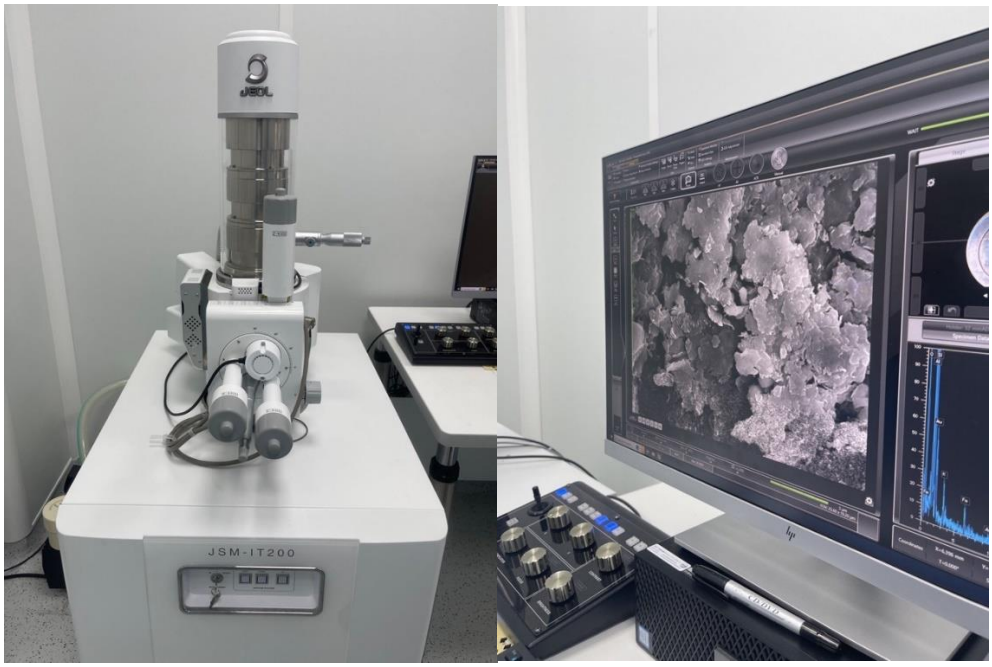

Figure 3-10 The Scanning Electron Microscope (SEM) JEOL JSM-IT200(LA).

3.7 Rheological measurements

Rheological characteristics of the prepared muds were examined in accordance with the API's approved procedure for preparing and evaluating drilling fluids (API Specifications 13B-1, 2009). Anton Paar Modular Compact Rheometer (MCR302) that was used during experiments is shown in Figure 3-11. This apparatus consists of measuring head, coupling for measuring system, flange ring, color display, softkeys, recessed grip, three adjustable feet and right-side cover. A concentric cylinder was installed to a rheometer for the measuring rheological properties. An integrated temperature control unit was used to regulate the temperature. After installing the rheometer according to manufacturer's guidelines and ensuring that everything works properly, the instrument was switched on and special software for MCR 302 was turned on. Freshly prepared smart drilling mud was placed inside the rheometer. The required temperature values were inserted. After thermal equilibrium was achieved, the measurement parameters were set up according to the software's manual. In this research work, the data was collected at constant speeds of 600, 300, 200, 100, 60, 30, 6, and 3 rpm, corresponding to Newtonian shear rates on the inner stationary cylinder of 1021.38, 510.67, 340.46, 170.23, 102.14, 51.069, 10.21, and 5.11 s^{-1}, respectively (Kelessidis & Maglione, 2008). The measurements were taken at temperatures of 25, 50, 75, and 100°C.

Figure 3-11. The MCR 302 Modular Compact Rheometer

The recorded shear stress and shear rate data were analyzed using the Herschel-Bulkley model. The model was fitted to the experimental data, and its fit was assessed by calculating the R^2 values and squared differences. Drilling fluid exhibiting nonlinear shear thinning behavior when yield stress is applied considered a non-Newtonian fluid. The results provided by this experiment were matched with the Herschel-Bulkley model to forecast the rheological behavior of the drilling fluid in presence of nanoparticles (Herschel & Bulkley, 1926). The mathematical expression of this model is as follows:

$$\tau = \tau_0 + k \times \dot{\gamma}^n \quad (1)$$

where τ is the shear stress measured in Pa, τ_0 is the yield point in Pa, k is the dimensionless consistency index, gamma $(\dot{\gamma})$ is the shear rate measured in $sec^{-1,}$ and n is the index representing the behavior of shear-thinning fluid flow.

The yield stress was determined from the rheograms by extrapolating shear stress-shear rate curve to a zero shear rate and a rheological model is then applied to fit the experimental data. The least square fit method (by Excel Solver) was used to derive the rheological parameters (K

and n). The coefficient of determination (R^2) and the sum of squared errors (Q^2) were used to evaluate the optimal fit between observed and predicted values. To determine the best fit, the regression coefficient (R^2) and the sum of squared errors (SQ^2) were calculated:

$$\Sigma Q^2 = \sum_{i=1}^{n}(x_i - \hat{x_i})^2 \quad (2)$$

where $x_i$the experimentally obtained value of is shear stress and $\hat{x_i}$ is the estimated value of shear stress by HB model.

Measured shear stresses were obtained in a form rheograms and were used to identify apparent viscosity (AV) and plastic viscosity (PV) under stabilized shear rates (γ) data from 511 s^{-1} to 1022 s^{-1}. The plastic viscosity and apparent viscosity were calculated by the Equations 3 and 4, respectively.

Plastic Viscosity (cP) = μ_p = 600 RPM reading-300 RPM reading ……. (3)

$$Apparent\ Viscosity\ (cp) = \mu_a = \frac{600\ RPM\ reading}{2} \quad (4)$$

4 Results and discussion

4.1 Characterization of NiO NPs

Figure 4-1 shows the SEM image of nickel oxide NPs. The high-resolution SEM analysis of NiO nanoparticles revealed surface features such as small pores and surface roughness, which can positively impact the filtration and rheological characteristics of drilling fluids. These features increase the surface area of the nanoparticles, facilitating the formation of a low-permeability filter cake for reduced fluid loss and improved wellbore stability. Additionally, the surface features enhance the interaction between the nanoparticles and the fluid medium, potentially altering the fluid's viscosity, and shear-thinning behavior, leading to better hole cleaning efficiency and suspension of cuttings and weighting agents.

The SEM analysis of NiO nanoparticles revealed the agglomeration phenomenon, where particles cluster together to form larger structures due to their high surface energy. This agglomeration can lead to uneven distribution in the drilling fluid, reduced surface area, and sedimentation, negatively impacting the fluid's rheological properties, filtration control, and wellbore stability. Images of NiO NPs obtained by TEM are shown in Figure 4-2. The analysis of TEM images demonstrated a relatively narrow size distribution, with most particles falling within the 18-24 nm range.

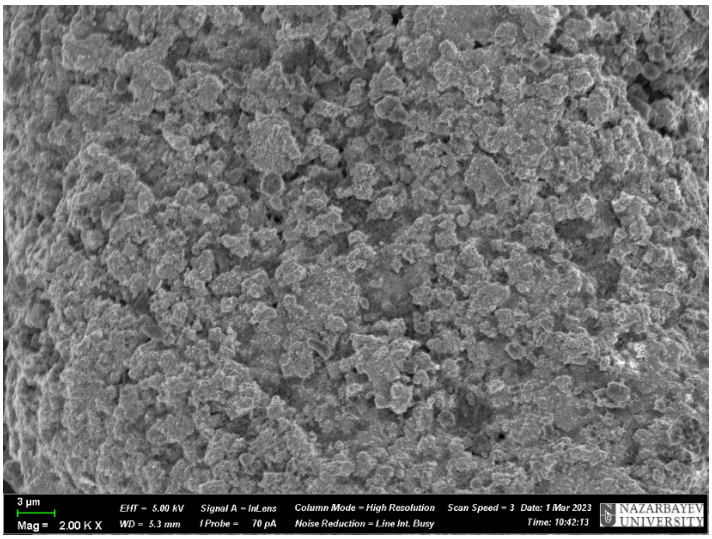

Figure 4-1. SEM of NiO nanoparticles under (X2000-3 µm magnification)

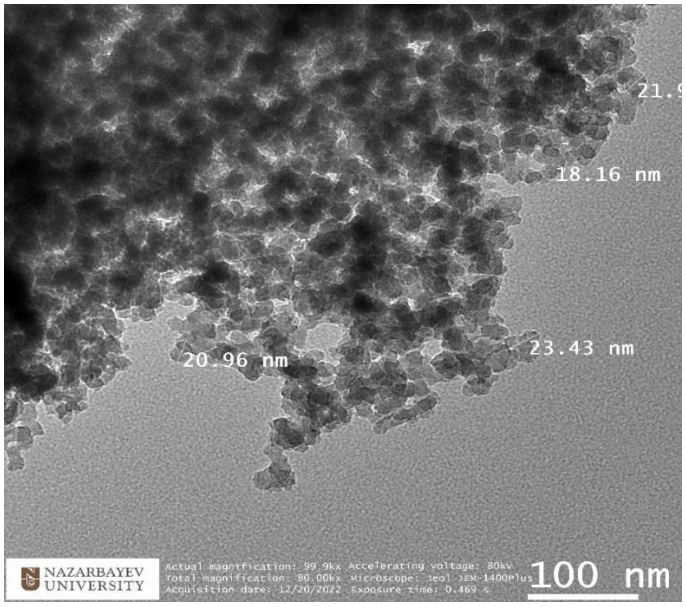

Figure 4-2. TEM analysis, particle size < 25 nm

4.2 Filtration measurements

4.2.1 *Thickness of filter cake*

Three different concentrations of 0.25%, 0.5% and 1.0% of NiO nanoparticles were used to study effect of NiO NPs on the thickness of a filter cake with reference to 7% bentonite water-based mud is shown in Table 4.2-1. Figure 4-3 demonstrates the experimental results on the effect of NiO concentration on filter cake thickness at a differential pressure of 500 psi and a temperature of 130°C. The results show that thickness of filter cake increased by 6.7% and 20.0% with increasing NiO NPs concentration up to 0.25% and 0.5%, respectively. The increase of the thickness can be explained by considering that with increasing the concentration of NPs results in a higher number of particles in a fluid, which are capable to form a thicker filter cake. In contrast, 1.0% concentration of NiO NPs resulted in an unexpected decrease in filter cake thickness by 10%. This phenomenon requires a possible investigation. One possible explanation is that NiO NPs reached its saturation limit, and this resulted in the formation of a thinner and rigid microstructure inside the filter cake.

Table 4.2-1. Effect of nanoparticles on thickness of filter cake

NiO concentration (wt. %)	Thickness of the Filter Cake (cm)	Percentage change of thickness with respect to 0%
0.000	0.30	–
0.250	0.32	+6.7
0.500	0.36	+20.0
1.000	0.27	−10

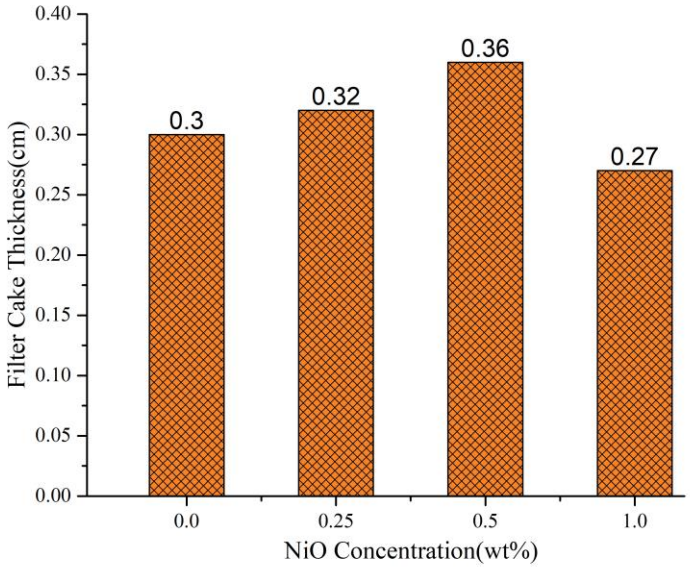

Figure 4-3. Effect of NiO concentration on filter cake thickness under HPHT conditions

4.2.2 *Filtration volume*

The effect of three different concentrations of 0.25%, 0.5%, and 1.0% of NiO NPs on the filtration volume with reference to 7% bentonite water-based mud is shown in Table 4.2-2. The 30-minutes cumulative filtrate volume under HPHT conditions are presented in Figure 4-4. The results show that 0.25% of NiO NPs reduced the fluid loss by 24.9%. However, increasing the concentration of NiO to 0.5% and 1.0% resulted in decrease of filtrate volume only by 8.7 and 7.4%, respectively. This decrease of fluid loss can be attributed to the formation of an efficient seal as a result of the blocking of the voids left by the coarse-sized particles and cracks (Ahmed Mansoor et al., 2021). 0.5% and 1.0% concentration of NiO nanoparticles showed worth filtration results due to NPs agglomeration and instability of a filter cake. Grouping of NiO NPs results in larger particles that can not plug pores of the filter cake and ceramic disk. Since 0.5% and 1.0% concentrations of NiO

nanoparticles did not perform as well as 0.25% concentrations, the concentration of 0.25% was concluded to be the optimal concentration.

Table 4.2-2. Effect of nanoparticles on cumulative filtrate volume

NiO concentration (wt. %)	Cumulative Filtrate volume 30 min (ml)	Percentage change of filtrate volume with respect to 0%
0.000	26.9	–
0.250	20.4	−24.9
0.500	24.6	−8.7
1.000	24.9	−7.4

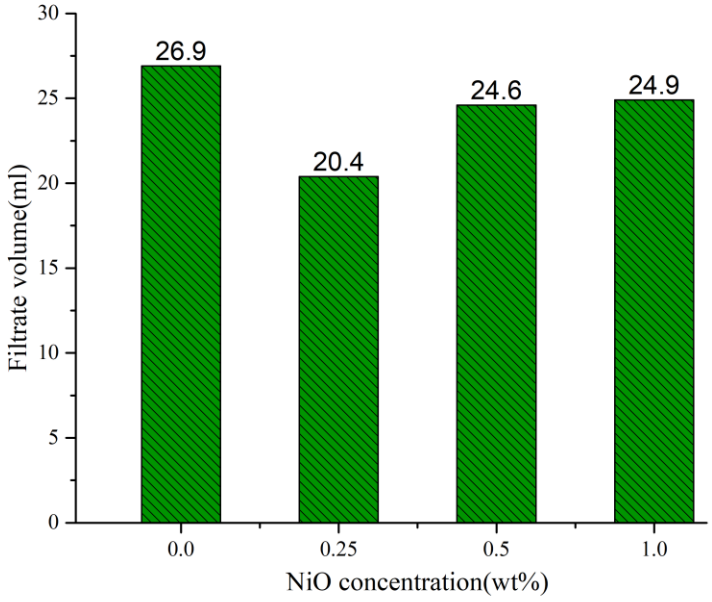

Figure 4-4. Effect of NiO concentration on 30 min filtrate volume under HPHT conditions

Table 4.2-3 show the filtrate volume collected at two-time intervals: 1 min and 7.5 min. Figure 4-5 shows the experimental results about the effect of NiO NPs' concentration on filtrate volume collected at 1 and 7.5 minutes at a differential pressure of 500 psi and a temperature of 130°C. In comparison with the base fluid, the filtration volume after 1 min is also known as spurt loss decreasing by 12.0% for the sample with 0.25% NiO. This shows that NiO NPs positively affect the formation of an initial layer that stops fluid loss. 0.25% of NiO NPs was also the best concentration for decreasing filtrate volume after 7.5 min by 9.5%.

Table 4.2-3. Effect of nanoparticles on filtrate volume 1 and 7 min

NiO concentration (wt. %)	Filtrate volume 1 min (Spurt loss) (ml)	Percentage change of filtrate volume with respect to 0%	Filtrate volume 7.5 min (ml)	Percentage change of filtrate volume with respect to 0%
0.000	2.2	–	8.1	–
0.250	1.9	−12.0	7.3	−9.5
0.500	2.1	−4.5	7.9	−2.7
1.000	2.1	−4.5	8.0	−1.4

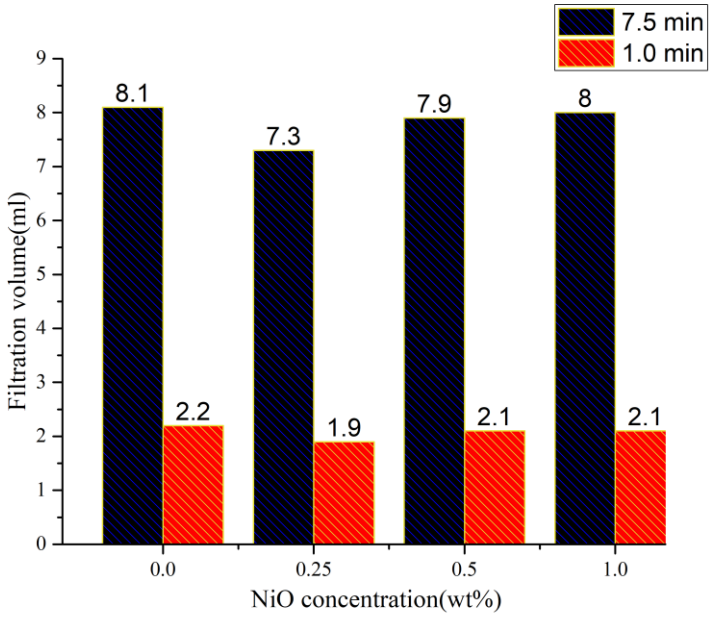

Figure 4-5. Effect of NiO concentration on 1 and 7.5 min filtrate volume under HPHT conditions

4.2.2.1 Filter cake appearance, morphology and elements

Figure 4-6 shows images of the filter cakes that changed based on the concentration of nanoparticles. Filter cakes have noticeable differences in color. In fact, color becomes darker with increasing NiO concentration. This effect becomes more prominent in Figure 4-7 that shows images of filter cakes after placing into the oven for 3 hours under 120°C in order to obtain SEM images. NiO nanoparticles have a black color. The fact that filter cakes get darker and darker means that nanoparticles did not penetrate through the ceramic disk.

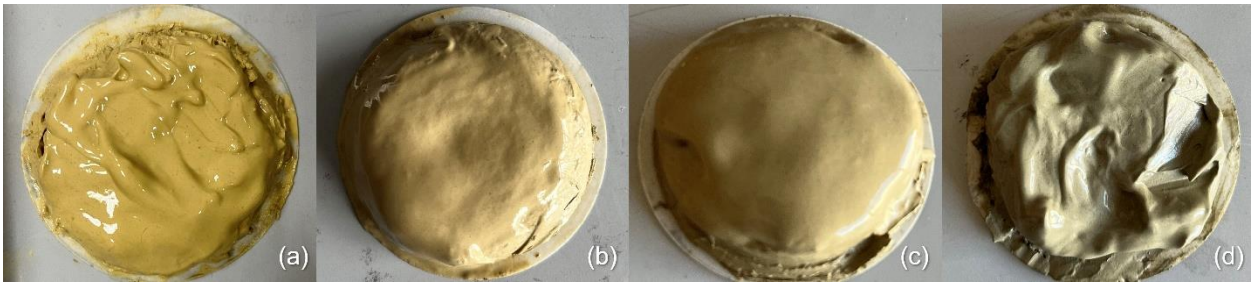

Figure 4-6. Images of Filter cakes with (a) 0% (b) 0.25% (c) 0.5% (d) 1% NiO concentration

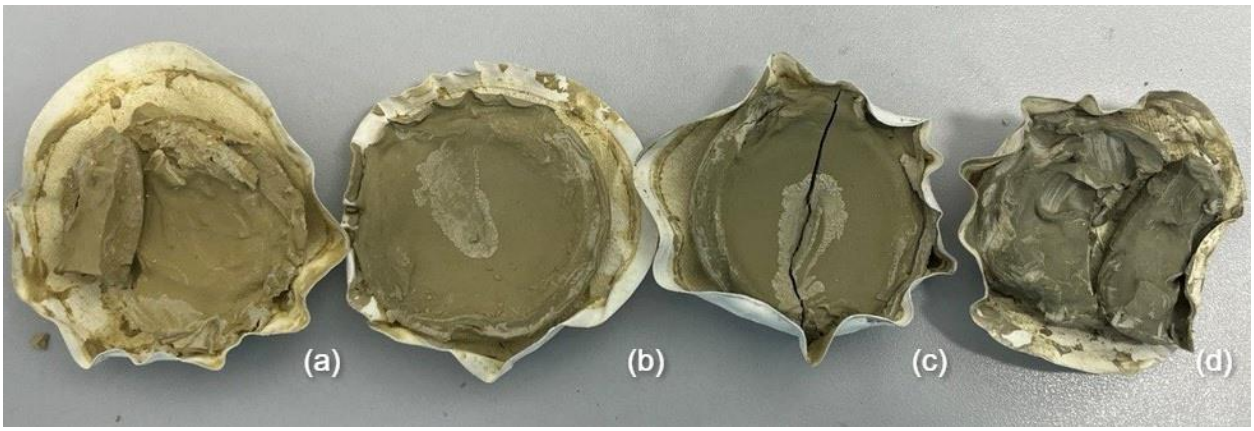

Figure 4-7. Filter cakes after heating with (a) 0% (b) 0.25% (c) 0.5% (d) 1% NiO concentration

The effect of NiO NPs concentration on the morphology of the filter cake was examined using SEM images. Figure 4-8 and Figure 4-9 shows filter cake SEM micrographs magnified by 950 and 5000 times, respectively. Bentonite particles have plate-like structures. That is how the presence of NPs on SEM images was differentiated and marked by using white squares. By comparing control sample and filter cakes with nanoparticles, it can be observed that NiO nanoparticles interact with bentonite particles, making denser and rougher filter cakes. As a result, the filter cake network is more connected forming chain-like structures and has fewer void spaces. Big pore throats are clearly seen in the microstructure of the filter cake without any nanoparticles in Figure 4-9 (a). Those pore throats significantly decrease the quality of a filter cake. Inefficiency of using higher concentrations (0.5% and 1.0%) of NiO can be explained by non-homogeneous distribution and agglomeration of the NPs shown in Figure 4-9 (c) (d).

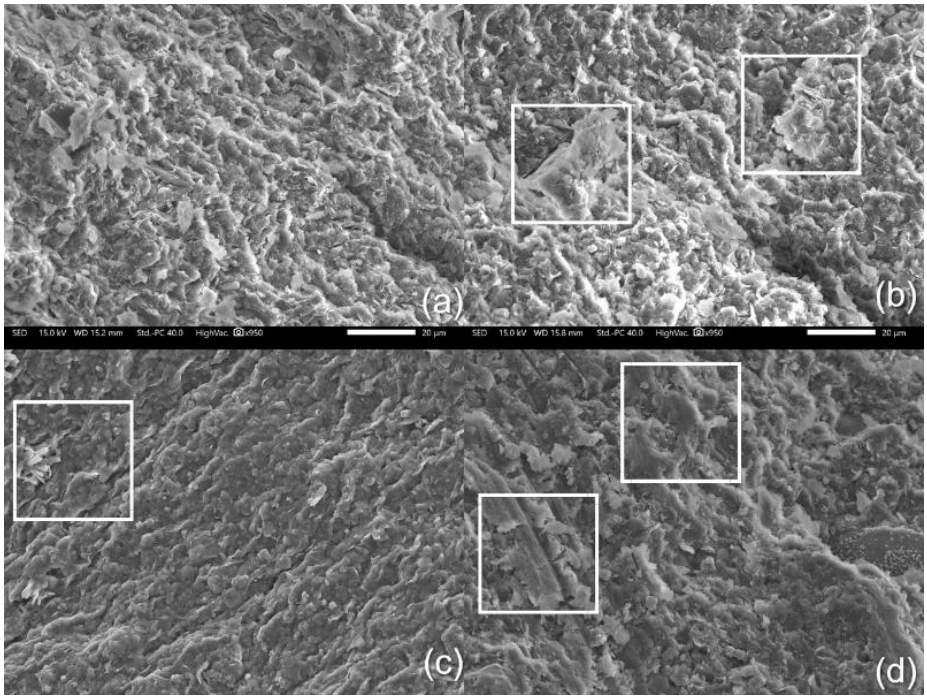

Figure 4-8. SEM images of filter cakes with (a) 0% (b) 0.25% (c) 0.5% (d) 1% NiO concentration (X950-20 μm magnification)

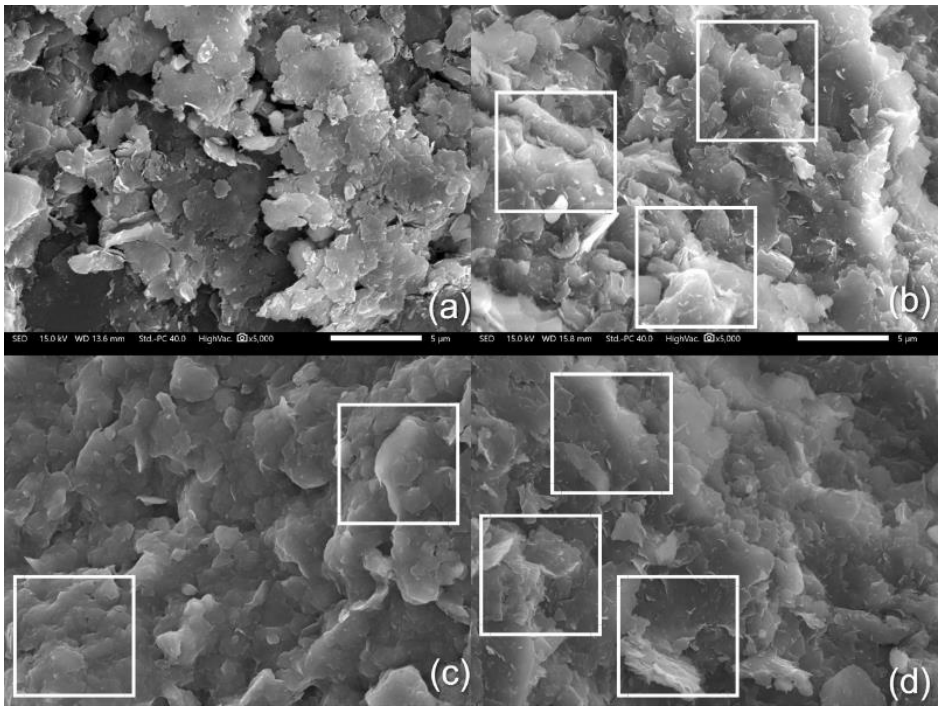

Figure 4-9. SEM images of filter cakes with (a) 0% (b) 0.25% (c) 0.5% (d) 1% NiO concentration (X5000-5 μm magnification)

Percentages in terms of elemental composition of the filter cakes was identified by the EDS micro-analysis. Results are shown on Figure 4-10. Due to the usage of bentonite, the EDS was able to determine the amounts of aluminum (Al) and silicon (Si). Si and Al are coming from a naturally occurring smectite clay belonging to the phyllosilicate 2:1 family that is composed of an Al^{3+} octahedral layer sandwiched between two Si^{4+} tetrahedral layers (Mahmoud et al., 2017). As expected increasing the concentration of NiO NPs increased the weight percent of Ni in filter cakes. Another interesting observation of Figure 4-10 is that the concentration of Mg, Ca and Fe slightly decreased. This can be explained by considering the dissociation of cations of bentonite particles.

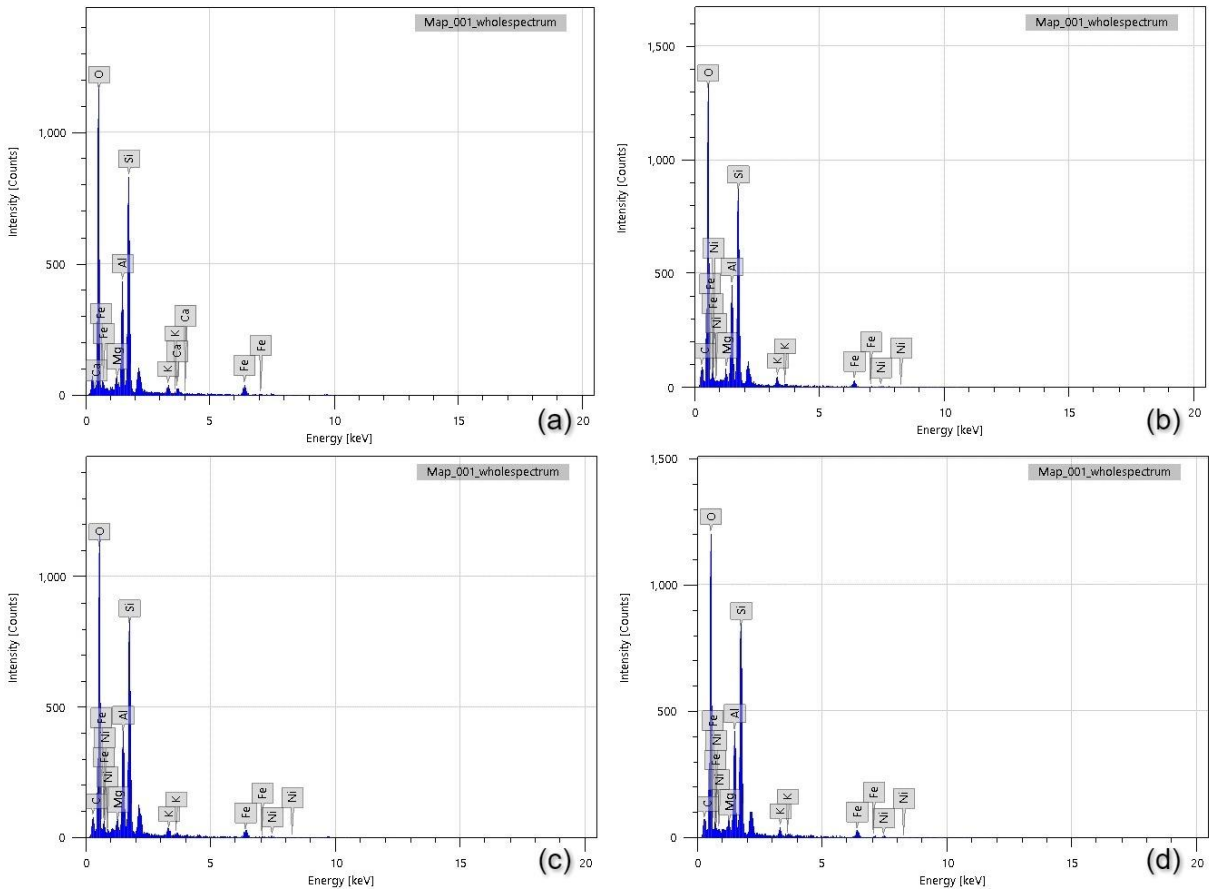

Figure 4-10. EDS elemental analysis of filter cake with (a) 0% (b) 0.25% (c) 0.5% (d) 1% NiO concentration

4.3 Rheological analysis

This study investigated the rheological characteristics of water-based drilling muds with varying nanoparticle concentrations at temperatures 25, 50, 75, and 100°C and ambient pressure using

Herschel-Bulkley model which is applied for non-Newtonian fluids. The following Figure 4-11 displays the rheograms of the base fluid without any addition of NiO nanoparticle at different temperatures. The Herschel-Bulkley model was used to fit the raw data at various temperatures, and the resulting rheological parameters for the base fluid are presented in Table 4.3-1. The experimental data aligns most accurately with the Herschel-Bulkley model, as evidenced by R^2 values surpassing 0.99 and the smallest Q^2 values observed for most of the scenarios. The yield stress was 3.422 Pa at room temperature. When the temperature increased to 50°C, the yield stress decreased to 2.745 Pa (-19.8%). However, at 75°C, the yield stress increased to 4.806 Pa (+40.4%), and the maximum yield stress value of 5.601 Pa was measured at 100°C (+63.5%), the highest tested temperature (Table 4.3-1). This observed trend can likely be ascribed to the phenomenon where, at elevated temperatures, individual bentonite particles clump together and create larger aggregates, subsequently resulting in a continuous gel-like structure that contributes to increased yield stress values (Vryzas et al., 2017). It is evident that at elevated temperatures, the flow consistency index (K) diminished, while the flow behavior index (n) increased (approaching the value of 1.0) at higher temperatures.

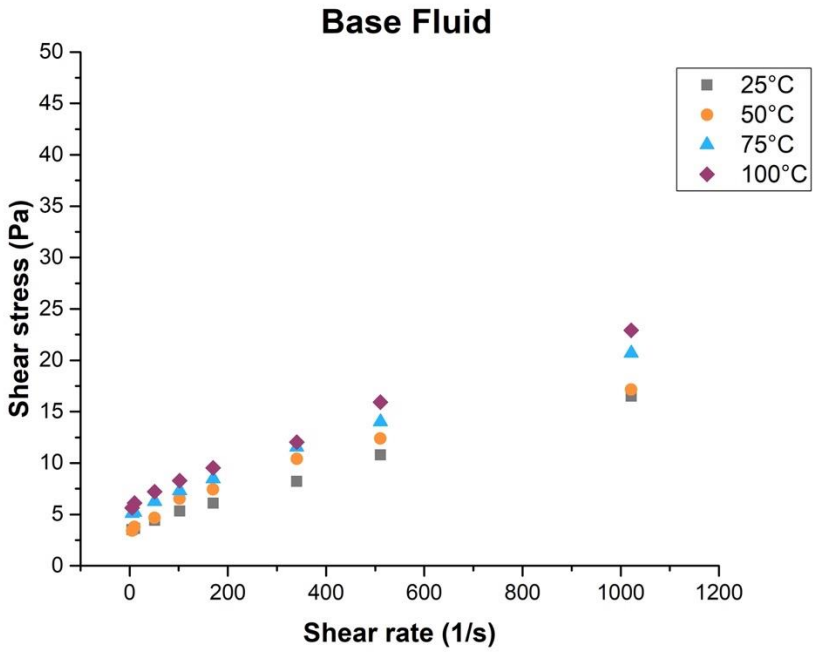

Figure 4-11. Rheograms for Base Fluid without NPs.

Table 4.3-1. Rheological parameters by Herschel-Bulkley model for base fluid.

	Herschel-Bulkley Model				
T (°C)	**τ_0 (Pa)**	**K (Pa·s^n)**	**n**	**R^2**	**$\sum Q^2$ (Pa^2)**
25	3.422	0.218	0.606	0.999	0.123
50	2.745	0.064	0.797	0.998	0.363
75	4.806	0.057	0.826	1.000	0.044
100	5.601	0.031	0.871	0.997	0.676

Enhancements in rheological properties at elevated temperatures were observed upon adding nickel oxide nanoparticles to the base fluid. Figures 4-12, 4-13 and 4-14 display the rheograms of drilling fluids containing 0.25, 0.5 and 1.0 wt.% NiO NPs at various temperatures, respectively. Displayed in Tables 4.3-2, 4.3-3 and 4.3-4 are the calculated rheological properties of drilling fluids with varying concentrations of nickel oxide nanoparticles (0.25, 0.5 and 1.0 wt.%) at distinct temperatures.

Addition of 0.25% NiO NPs resulted in higher yield stress values compared to the base fluid (BF) at all tested temperatures, this concentration of NiO NPs represents the greatest enhancement in yield stress among all examined nanoparticle concentrations. More specifically, the yield stress values were 6.913 Pa at 25°C (+102.0%), 8.584 Pa at 50°C (+212.3%), 8.734 Pa at 75°C (+81.7%), and 9.527 Pa at 100°C (+70.1%) (see Table 4-12). This is likely due to the NiO NPs forming sizable aggregates and contributing to the development of interparticle connections, resulting in a substantial elevation in the yield stress of these suspensions when compared to pure bentonite suspensions, leading to the formation of a more robust gel-like structure. The flow consistency index (K) and the flow behavior index (n) displayed a similar trend as the base fluid, showing a decrease in K values and an increase in n values with rising temperatures. The HB model once again delivers an outstanding fit, with high R^2 values.

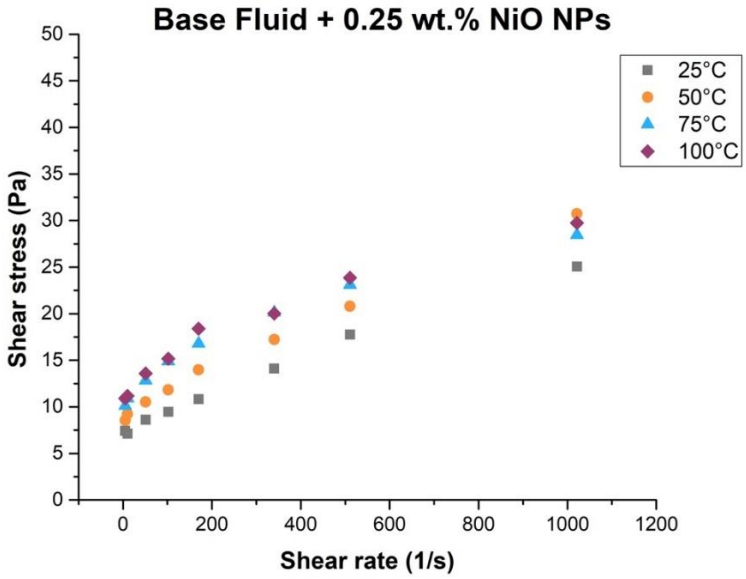

Figure 4-12. Rheograms for Mud+0.25 wt.%.

Table 4.3-2. Rheological parameters by Herschel-Bulkley model for Mud+0.25 wt.%.

	Herschel-Bulkley Model				
T (°C)	**τ_0 (Pa)**	**K (Pa·s^n)**	**n**	**R^2**	**$\sum Q^2$ (Pa^2)**
25	6.913	0.603	0.504	0.998	0.591
50	8.584	0.525	0.527	0.999	0.374
75	8.734	0.071	0.826	0.999	0.293
100	9.527	0.06	0.829	0.993	2.004

When 0.5% NiO NPs were added, the yield stress values showed an increase at 50°C and 75°C compared to the BF, with 7.168 Pa at 50°C (+161.3%) and 8.005 Pa at 75°C (+66.4%). However, the yield stress values at 25°C and 100°C were 4.715 Pa (+37.8%) and 8.627 Pa (+54.0%), which were higher than the BF but lower than those of the 0.25% NiO NPs sample. This suggests that the higher concentration of NiO NPs could have caused some degree of particle aggregation, resulting in a less significant increase in yield stress values compared to the 0.25% NiO NPs sample.

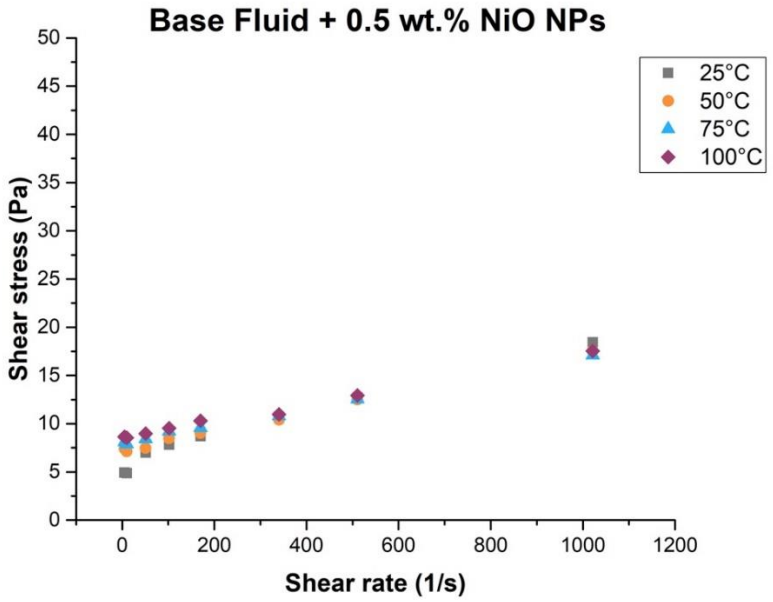

Figure 4-13. Rheograms for Mud+0.5 wt.%.

Table 4.3-3. Rheological parameters by Herschel-Bulkley model for Mud+0.5 wt.%.

	Herschel-Bulkley Model				
T (°C)	**τ_0 (Pa)**	**K (Pa·s^n)**	**n**	**R^2**	**$\sum Q^2$ (Pa^2)**
25	4.715	0.114	0.689	0.994	0.916
50	7.168	0.011	0.988	0.997	0.253
75	8.005	0.009	1.001	0.997	0.210
100	8.627	0.005	1.002	0.995	0.353

The addition of 1.0% NiO NPs led to increased yield stress values at 50°C and 75°C compared to the BF, with 4.152 Pa at 50°C (+51.2%) and 4.430 Pa at 75°C (-7.8%). However, the yield stress values at 25°C and 100°C were 4.112 Pa (+20.1%) and 3.717 Pa (-33.6%), which were lower than those of the 0.5% NiO NPs sample. This indicates that the higher concentration of NiO NPs might have caused significant particle aggregation, thereby reducing the effectiveness of the NPs in enhancing the yield stress values.

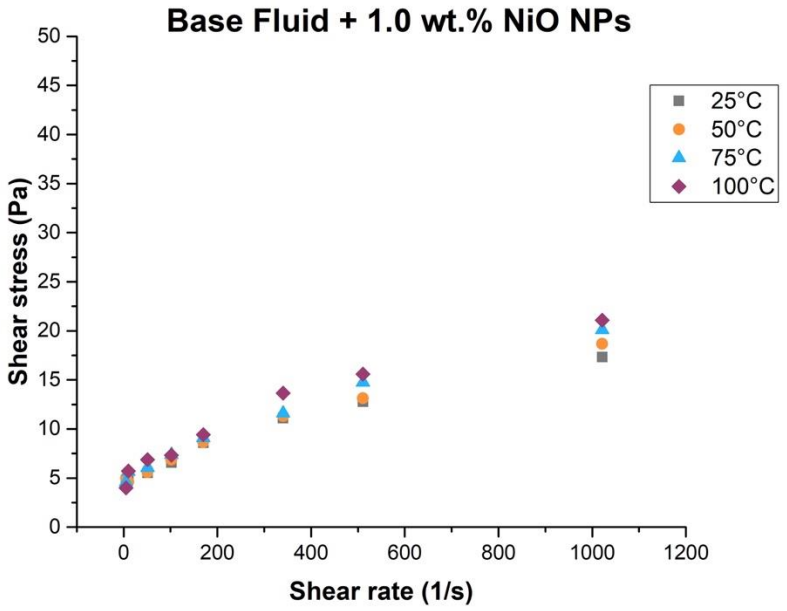

Figure 4-14. Rheograms for Mud+1.0 wt.%.

Table 4.3-4. Rheological parameters by Herschel-Bulkley model for Mud+1.0 wt.%.

	Herschel-Bulkley Model				
T (°C)	**τ_0 (Pa)**	**K (Pa·s^n)**	**n**	**R^2**	**$\sum Q^2$ (Pa^2)**
25	4.112	0.29	0.593	0.993	0.959
50	4.152	0.152	0.646	0.996	0.618
75	4.430	0.130	0.688	0.995	0.948
100	3.717	0.124	0.694	0.989	2.537

The addition of NiO NPs led to an increase in yield stress values compared to the BF, with the most significant improvement observed for the 0.25% NiO NPs sample. The flow consistency index (K) showed lower values for the samples containing NiO NPs compared to the BF, while the flow behavior index (n) generally increased with increasing temperature. This suggests that NiO NPs affect the rheological characteristics of the drilling mud, leading to changes in its flow behavior under various temperature conditions.

The highest yield stress was observed in the sample containing 0.25 wt% NiO nanoparticles which is illustrated in Figure 4-15. The yield stress increased by up to 70% compared to the base fluid, indicating that incorporating NiO nanoparticles at this concentration enhances the drilling mud's performance under HPHT conditions. This enhancement can be attributed to several factors, including sstrengthened interactions between NiO nanoparticles and the base fluid, resulting in a more robust structure, and potential formation of a network-like structure within the drilling mud, which reinforces the overall rheological properties. Higher yield stress improves the suspension and transportation of drill cuttings, preventing their accumulation and reducing the risk of stuck pipe incidents.

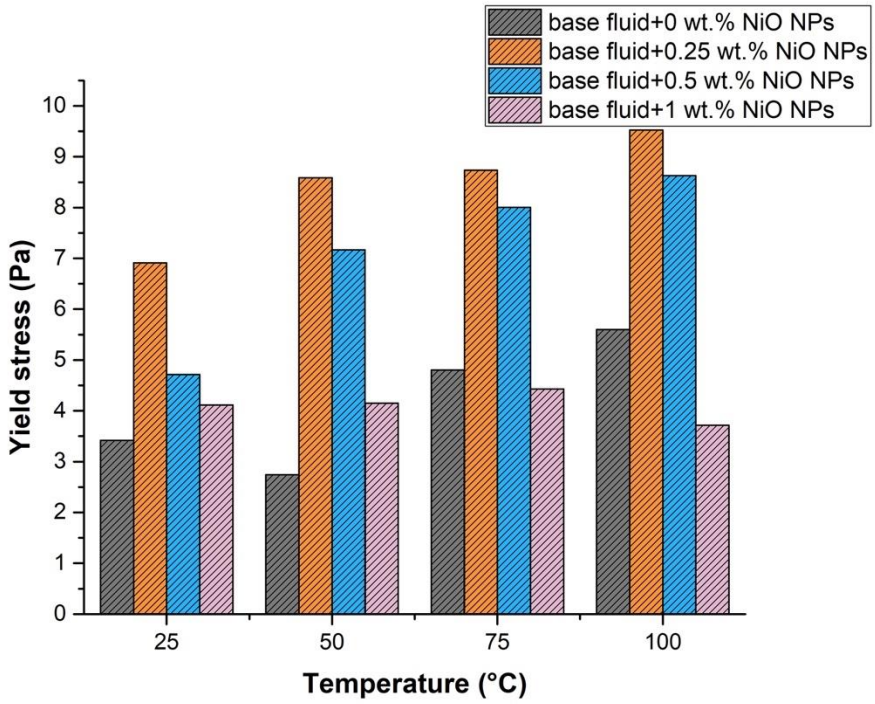

Figure 4-15. Yield stress values for different concentrations of NiO NPs compared to base fluid at different temperatures.

The apparent viscosity values at 100°C for the base fluid and the fluid with various concentrations of NiO NPs (0.25 wt.%, 0.5 wt.%, and 1.0 wt.%) are shown in Figure 4-16. The experimental results showed that tested samples displayed shear-thinning characteristics (a decrease in apparent viscosity with increasing shear rate) as shown in Figure 4-16 and 4-17. The greatest increase in apparent viscosity was observed for the 0.25 wt.% NP concentration, with values ranging from 0.01 to 0.013 Pa·s at the highest shear rate of 1021.38 (1/s). A drilling fluid

with high apparent viscosity can help maintain better control of downhole pressures, which is essential for preventing kicks, lost circulation, and other drilling hazards related to pressure management. The lowest increase was observed for the 1.0 wt.% NP concentration, with values ranging from 0.009 to 0.012 Pa·s at the same shear rate. The 0.25 wt.% concentration of nanoparticles resulted in a more consistent viscosity at higher temperatures, indicating that the nanoparticles can help prevent the decrease in viscosity that normally occurs with increasing temperature. This suggests that the nanoparticles can produce similar rheological behavior across different temperatures.

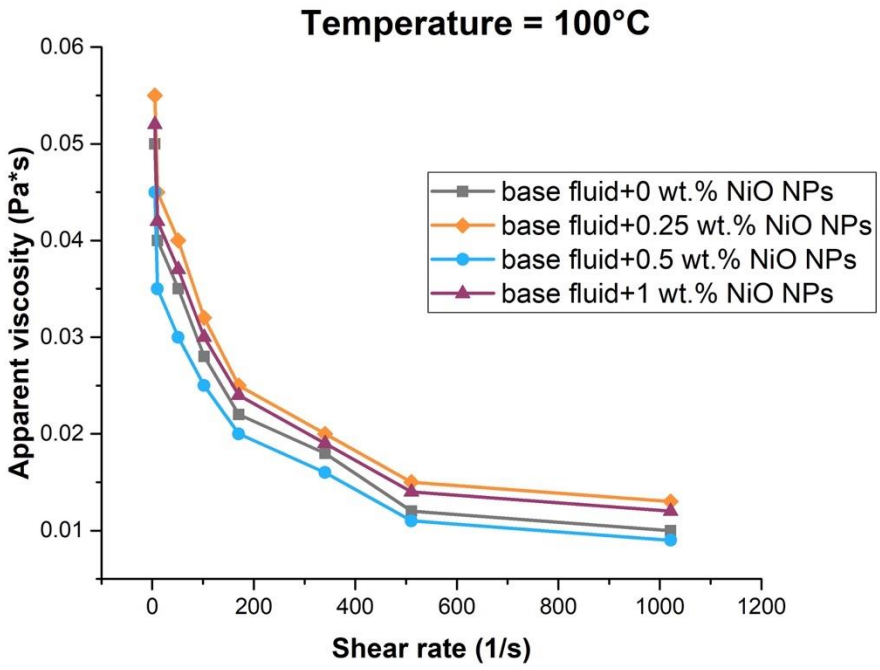

Figure 4-16. Apparent viscosity values as a function of shear rate for different concentrations at 100°C

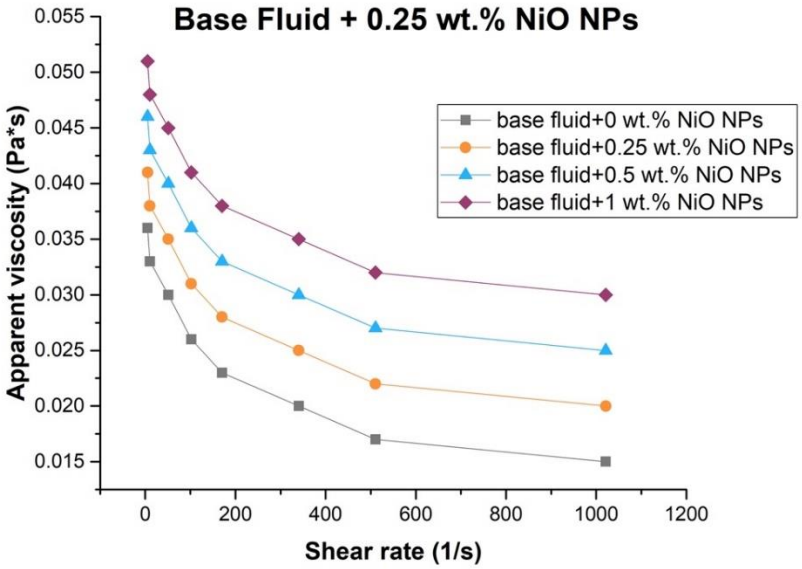

Figure 4-17. Apparent viscosity values as a function of shear rate at different temperatures for 0.25 wt.% NiO NPs

The Figure 4-18 illustrates the plastic viscosity values for each sample at different temperatures. The plastic viscosity values for the base fluid were relatively consistent across all temperatures, ranging from 3-4 (mPa·s). The addition of NiO NPs at a concentration of 0.25 wt% resulted in an increase in plastic viscosity values at all temperatures, with the highest increase seen at 75°C. At 0.5 wt% and 1.0 wt% NiO NP concentrations, the plastic viscosity values were generally lower than the base fluid values, although there was some variation depending on the temperature. Specifically, at 25°C and 50°C, the plastic viscosity values were lowest for the 0.5 wt% and 1.0 wt% NiO NP concentrations, while at 75°C and 100°C, the plastic viscosity values were similar or slightly higher than the base fluid values. Overall, these results suggest that the addition of NiO NPs at 0.25 wt% can significantly increase the plastic viscosity of the base fluid at all temperatures, while higher concentrations of NiO NPs may not be as effective and can even decrease the plastic viscosity depending on the temperature. A drilling fluid with high plastic viscosity can help reduce fluid loss into permeable formations, as it forms a more effective filter cake on the wellbore walls. This can help maintain the fluid's properties and reduce the risk of formation damage. Also, a drilling fluid with high plastic viscosity can provide better wellbore stability by exerting a more uniform force on the wellbore walls. This reduces the risk of wellbore collapse or caving during drilling operations.

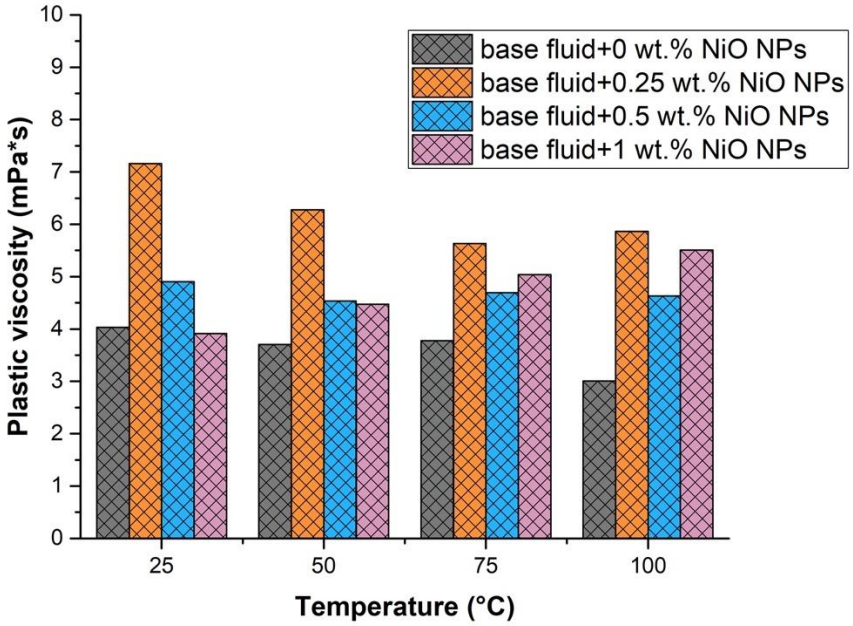

Figure 4-18. Plastic viscosity values for samples at different temperatures.

Even after adding NPs, the samples continue to exhibit shear-thinning behavior, but their rheological performance improves at higher NP concentrations, particularly for the concentration of 0.25 wt.% NiO nanoparticles. These advantages are significant for the design of drilling fluids, as the behavior of the fluid under normal conditions can reflect its behavior under downhole conditions. A drilling fluid that exhibits consistent behavior at HPHT conditions could be highly beneficial and find potential applications, as its viscosity would be dependent solely on shear rate rather than on pressure and temperature.

5 Conclusions

In summary, NiO NPs produced satisfactory results under HPHT conditions. The filtrate volume and filter cake thickness were lower in the test samples with NiO NPs than in the control sample. The reason for this is that the special properties of NiO NPs can create rigid networks with bentonite particles. Characterization by using SEM, TEM proved that NiO NPs have effective size and morphology for improving rheologic and filtration properties of WBM. Especially, 0.25% concentration of NiO NPs achieved the biggest reduction filtration loss of 24.9%, followed by 0.5% and 1.0% concentrations of NiO with reductions of 8.7% and 7.4%, respectively. SEM analyses showed that addition of NiO NPs changed morphology of filter cakes to more uniform and less permeable structures.

The presence of NiO NPs had a notable influence on the rheological properties of the samples, and the 0.25 wt.% is the optimal concentration of NiO NPs which led to enhanced performance, particularly in terms of increased yield stress, plastic viscosity, and apparent viscosity. The Herschel-Bulkley model offered an outstanding fit for characterizing the flow behavior of our drilling fluid samples at atmospheric pressure and temperatures up to 100°C. Based on the experimental results, the addition of NiO NPs to the drilling fluid improved its apparent viscosity at higher temperatures and resulted in a more stable viscosity behavior across different temperatures. Additionally, the plastic viscosity values showed an increase with increasing nanoparticle concentration, indicating that NiO NPs can enhance the rheological performance of the drilling fluid. These findings suggest that NiO NPs have the potential to be used as effective additives in drilling fluid design for high temperature and high-pressure applications.

References

Abdo, J., & Haneef, M. D. (2012). Nano-Enhanced Drilling Fluids: Pioneering Approach to Overcome Uncompromising Drilling Problems. *Journal of Energy Resources Technology*, *134*(1). https://doi.org/10.1115/1.4005244

Abdo, J., & Haneef, M. D. (2013). Clay nanoparticles modified drilling fluids for drilling of deep hydrocarbon wells. *Applied Clay Science*, *86*, 76–82. https://doi.org/10.1016/J.CLAY.2013.10.017

Aftab, A., Ali, M., Sahito, M. F., Mohanty, U. S., Jha, N. K., Akhondzadeh, H., Azhar, M. R., Ismail, A. R., Keshavarz, A., & Iglauer, S. (2020). Environmental Friendliness and High Performance of Multifunctional Tween 80/ZnO-Nanoparticles-Added Water-Based Drilling Fluid: An Experimental Approach. *ACS Sustainable Chemistry and Engineering*, *8*(30), 11224–11243. https://doi.org/10.1021/acssuschemeng.0c02661

Aftab, A., Ismail, A. R., Ibupoto, Z. H., Akeiber, H., & Malghani, M. G. K. (2017). Nanoparticles based drilling muds a solution to drill elevated temperature wells: A review. In *Renewable and Sustainable Energy Reviews* (Vol. 76, pp. 1301–1313). Elsevier Ltd. https://doi.org/10.1016/j.rser.2017.03.050

Agwu, O. E., Akpabio, J. U., Ekpenyong, M. E., Inyang, U. G., Asuquo, D. E., Eyoh, I. J., & Adeoye, O. S. (2021). A comprehensive review of laboratory, field and modelling studies on drilling mud rheology in high temperature high pressure (HTHP) conditions. In *Journal of Natural Gas Science and Engineering* (Vol. 94). Elsevier B.V. https://doi.org/10.1016/j.jngse.2021.104046

Ahmed Mansoor, H. H., Devarapu, S. R., Samuel, R., Sharma, T., & Ponmani, S. (2021). Experimental investigation of aloe-vera-based cuo nanofluid as a novel additive in improving the rheological and filtration properties of water-based drilling fluid. *SPE Drilling and Completion*, *36*(3), 542–551. https://doi.org/10.2118/205004-PA

Albajalan, A. R., & Haias, H. K. (2021). Evaluation of the Performance of Conventional Water-Based Mud Characteristics by Applying Zinc Oxide and Silica Dioxide Nanoparticle Materials for a Selected Well in the Kurdistan/Iraq Oil Field. *Advances in Materials Science and Engineering*, *2021*. https://doi.org/10.1155/2021/4376366

Ali, J. A., Hamadamin, A. B., Ahmed, S. M., Mahmood, B. S., Sajadi, S. M., & Manshad, A. K. (2022). Synergistic Effect of Nanoinhibitive Drilling Fluid on the Shale Swelling Performance at High Temperature and High Pressure. *Energy and Fuels*, *36*(4), 1996–2006. https://doi.org/10.1021/ACS.ENERGYFUELS.1C03804/ASSET/IMAGES/LARGE/EF1C03804_0013.JPEG

Ali, M., Jarni, H. H., Aftab, A., Ismail, A. R., Saady, N. M. C., Sahito, M. F., Keshavarz, A., Iglauer, S., & Sarmadivaleh, M. (2020a). Nanomaterial-Based Drilling Fluids for Exploitation of Unconventional Reservoirs: A Review. *Energies 2020, Vol. 13, Page 3417*, *13*(13), 3417. https://doi.org/10.3390/EN13133417

Ali, M., Jarni, H. H., Aftab, A., Ismail, A. R., Saady, N. M. C., Sahito, M. F., Keshavarz, A., Iglauer, S., & Sarmadivaleh, M. (2020b). Nanomaterial-Based Drilling Fluids for Exploitation of Unconventional Reservoirs: A Review. *Energies 2020, Vol. 13, Page 3417*, *13*(13), 3417. https://doi.org/10.3390/EN13133417

Al-Saba, M. T., Al Fadhli, A., Marafi, A., Hussain, A., Bander, F., & Al Dushaishi, M. F. (2018). Application of Nanoparticles in Improving Rheological Properties of Water Based Drilling Fluids. *Society of Petroleum Engineers - SPE Kingdom of Saudi Arabia Annual*

Technical Symposium and Exhibition 2018, SATS 2018, 23–26. https://doi.org/10.2118/192239-MS

Al-Shargabi, M., Davoodi, S., Wood, D. A., Al-Musai, A., Rukavishnikov, V. S., & Minaev, K. M. (2022). Nanoparticle applications as beneficial oil and gas drilling fluid additives: A review. In *Journal of Molecular Liquids* (Vol. 352). Elsevier B.V. https://doi.org/10.1016/j.molliq.2022.118725

Al-Yasiri, M. S., & Al-Sallami, W. T. (2015). How the Drilling Fluids Can be Made More Efficient by Using Nanomaterials. *American Journal of Nano Research and Applications*, *3*(3), 41–45. https://doi.org/10.11648/j.nano.20150303.12

Al-Yasiri, M., & Wen, D. (2019). Gr-Al2O3 Nanoparticles-Based Multifunctional Drilling Fluid. *Industrial and Engineering Chemistry Research*, *58*(23), 10084–10091. https://doi.org/10.1021/acs.iecr.9b00896

Amanullah, M., Al-Tahini, A. M., & Aramco, S. (2009). *Nano-Technology – Its Significance in Smart Fluid Development for Oil and Gas Field Application*. http://onepetro.org/SPESATS/proceedings-pdf/09TSSA/All-09TSSA/SPE-126102-MS/2723877/spe-126102-ms.pdf/1

Amanullah, M., & Yu, L. (2005). Environment friendly fluid loss additives to protect the marine environment from the detrimental effect of mud additives. *Journal of Petroleum Science and Engineering*, *48*(3–4), 199–208. https://doi.org/10.1016/J.PETROL.2005.06.013

An, Y. X., Qu, W. J., Yu, P. Z., & Lü, J. G. (2018). The assembly of a composite based on nano-sheet graphene oxide and montmorillonite. *Petroleum Science*, *15*(2), 366–374. https://doi.org/10.1007/s12182-018-0216-3

Ao, T., Yang, L., Xie, C., Jiang, G., Wang, G., Liu, Z., & He, X. (2021). Zwitterionic Silica-Based Hybrid Nanoparticles for Filtration Control in Oil Drilling Conditions. *ACS Applied Nano Materials*, *4*(10), 11052–11062. https://doi.org/10.1021/acsanm.1c02504

API Specifications 13B-1. (2009). *Recommended Practice for Field Testing Water-based Drilling Fluids* (Fourth). API.

Bayat, A. E., Jalalat Moghanloo, P., Piroozian, A., & Rafati, R. (2018). Experimental investigation of rheological and filtration properties of water-based drilling fluids in presence of various nanoparticles. *Colloids and Surfaces A: Physicochemical and Engineering Aspects*, *555*, 256–263. https://doi.org/10.1016/j.colsurfa.2018.07.001

Bayat, A. E., & Shams, R. (2019a). Appraising the impacts of SiO2, ZnO and TiO2 nanoparticles on rheological properties and shale inhibition of water-based drilling muds. *Colloids and Surfaces A: Physicochemical and Engineering Aspects*, *581*, 123792. https://doi.org/10.1016/J.COLSURFA.2019.123792

Bayat, A. E., & Shams, R. (2019b). Appraising the impacts of SiO2, ZnO and TiO2 nanoparticles on rheological properties and shale inhibition of water-based drilling muds. *Colloids and Surfaces A: Physicochemical and Engineering Aspects*, *581*. https://doi.org/10.1016/j.colsurfa.2019.123792

Bég, O. A., Espinoza, D. E. S., Kadir, A., Shamshuddin, M., & Sohail, A. (2018). Experimental study of improved rheology and lubricity of drilling fluids enhanced with nano-particles. *Applied Nanoscience (Switzerland)*, *8*(5), 1069–1090. https://doi.org/10.1007/S13204-018-0746-4/TABLES/28

Chang, X., Sun, J., Xu, Z., Lv, K., Dai, Z., Zhang, F., Huang, X., & Liu, J. (2019). Synthesis of a novel environment-friendly filtration reducer and its application in water-based drilling

fluids. *Colloids and Surfaces A: Physicochemical and Engineering Aspects*, *568*, 284–293. https://doi.org/10.1016/J.COLSURFA.2019.01.055

Cheng, R., Lei, Z., Bai, Y., Zhang, J., Hao, H., & Xie, G. (2022). Preparation of the Tetrameric Poly(VS-St-BMA-BA) Nano-Plugging Agent and Its Plugging Mechanism in Water-Based Drilling Fluids. *ACS Omega*, *7*(32), 28304–28312. https://doi.org/10.1021/ACSOMEGA.2C02784/ASSET/IMAGES/MEDIUM/AO2C02784_M001.GIF

Cheraghian, G. (2021). Nanoparticles in drilling fluid: A review of the state-of-the-art. *Journal of Materials Research and Technology*, *13*, 737–753. https://doi.org/10.1016/j.jmrt.2021.04.089

Crucho, C. I. C., & Barros, M. T. (2017). Polymeric nanoparticles: A study on the preparation variables and characterization methods. In *Materials Science and Engineering C* (Vol. 80, pp. 771–784). Elsevier Ltd. https://doi.org/10.1016/j.msec.2017.06.004

Davoodi, S., Ramazani S.A., A., Jamshidi, S., & Fellah Jahromi, A. (2018). A novel field applicable mud formula with enhanced fluid loss properties in High Pressure-High Temperature well condition containing pistachio shell powder. *Journal of Petroleum Science and Engineering*, *162*, 378–385. https://doi.org/10.1016/J.PETROL.2017.12.059

Edalatfar, M., Yazdani, F., & Salehi, M. B. (2021). Synthesis and identification of ZnTiO3 nanoparticles as a rheology modifier additive in water-based drilling mud. *Journal of Petroleum Science and Engineering*, *201*. https://doi.org/10.1016/J.PETROL.2021.108415

El-Masry, J. F., Bou-Hamdan, K. F., Abbas, A. H., & Martyushev, D. A. (2023). A Comprehensive Review on Utilizing Nanomaterials in Enhanced Oil Recovery Applications. In *Energies* (Vol. 16, Issue 2). MDPI. https://doi.org/10.3390/en16020691

Fakoya, M. F., & Shah, S. N. (2014). *Enhancement of Filtration Properties in Surfactant-Based and Polymeric Fluids by Nanoparticles*. http://onepetro.org/SPEERM/proceedings-pdf/14ERM/All-14ERM/SPE-171029-MS/1513626/spe-171029-ms.pdf/1

Fazelabdolabadi, B., Khodadadi, A. A., & Sedaghatzadeh, M. (2015). Thermal and rheological properties improvement of drilling fluids using functionalized carbon nanotubes. *Applied Nanoscience (Switzerland)*, *5*(6), 651–659. https://doi.org/10.1007/s13204-014-0359-5

Felix, O., Nwaogazie, I. L., Akaranta, O., & Abu, G. O. (2018). Removal of Heavy Metals In Spent Synthetic-Based Drilling Mud Using Nano Zero-Valent Iron (nZVI). *Article in Journal of Scientific Research and Reports*, *21*(3), 1–11. https://doi.org/10.9734/JSRR/2018/45675

Gautam, S., Guria, C., & Rajak, V. K. (2022). A state of the art review on the performance of high-pressure and high-temperature drilling fluids: Towards understanding the structure-property relationship of drilling fluid additives. In *Journal of Petroleum Science and Engineering* (Vol. 213). Elsevier B.V. https://doi.org/10.1016/j.petrol.2022.110318

Gavignet, A. A., & Wick, C. J. (1987). COMPUTER PROCESSING IMPROVES HYDRAULICS OPTIMIZATION WITH NEW METHODS. *SPE Drilling Engineering*, *2*(4), 309–315. https://doi.org/10.2118/14774-PA

Hajiabadi, S. H., Aghaei, H., Kalateh-Aghamohammadi, M., & Shorgasthi, M. (2020). An overview on the significance of carbon-based nanomaterials in upstream oil and gas industry. In *Journal of Petroleum Science and Engineering* (Vol. 186). Elsevier B.V. https://doi.org/10.1016/j.petrol.2019.106783

Hamad, B. A., Xu, M., & Liu, W. (2019). Performance of environmentally friendly silica nanoparticles-enhanced drilling mud from sugarcane bagasse.

Https://Doi.Org/10.1080/02726351.2019.1675835, *39*(2), 168–179. https://doi.org/10.1080/02726351.2019.1675835

Herschel, W. H., & Bulkley, R. (1926). Konsistenzmessungen von Gummi-Benzollösungen. *Kolloid-Zeitschrift 1926 39:4*, *39*(4), 291–300. https://doi.org/10.1007/BF01432034

Hoberock, L. L., & Bratcher, G. J. (1998). Dynamic Differential Pressure Effects on Drilling of Permeable Formations. *Journal of Energy Resources Technology*, *120*(2), 118–123. https://doi.org/10.1115/1.2795021

Ibrahim, M. A., Jaafar, M. Z., Md Yusof, M. A., & Idris, A. K. (2022). A review on the effect of nanoparticle in drilling fluid on filtration and formation damage. In *Journal of Petroleum Science and Engineering* (Vol. 217). Elsevier B.V. https://doi.org/10.1016/j.petrol.2022.110922

Ikram, R., Jan, B. M., Vejpravova, J., Choudhary, M. I., & Chowdhury, Z. Z. (n.d.). *Recent Advances of Graphene-Derived Nanocomposites in Water-Based Drilling Fluids*. https://doi.org/10.3390/nano10102004

Ismail, A. R., Aftab, A., Ibupoto, Z. H., & Zolkifile, N. (2016). The novel approach for the enhancement of rheological properties of water-based drilling fluids by using multi-walled carbon nanotube, nanosilica and glass beads. *Journal of Petroleum Science and Engineering*, *139*, 264–275. https://doi.org/10.1016/J.PETROL.2016.01.036

Jia, X., Zhao, X., Chen, B., Egwu, S. B., & Huang, Z. (2022). Polyanionic cellulose/hydrophilic monomer copolymer grafted silica nanocomposites as HTHP drilling fluid-loss control agent for water-based drilling fluids. *Applied Surface Science*, *578*. https://doi.org/10.1016/j.apsusc.2021.152089

Katende, A., Boyou, N. V., Ismail, I., Chung, D. Z., Sagala, F., Hussein, N., & Ismail, M. S. (2019). Improving the performance of oil based mud and water based mud in a high temperature hole using nanosilica nanoparticles. *Colloids and Surfaces A: Physicochemical and Engineering Aspects*, *577*, 645–673. https://doi.org/10.1016/J.COLSURFA.2019.05.088

Kazemi-Beydokhti, A., & Hajiabadi, S. H. (2018). Rheological investigation of smart polymer/carbon nanotube complex on properties of water-based drilling fluids. *Colloids and Surfaces A: Physicochemical and Engineering Aspects*, *556*, 23–29. https://doi.org/10.1016/j.colsurfa.2018.07.058

Kelessidis, V. C., & Maglione, R. (2008). Yield stress of water–bentonite dispersions. *Colloids and Surfaces A: Physicochemical and Engineering Aspects*, *318*(1–3), 217–226. https://doi.org/10.1016/J.COLSURFA.2007.12.050

Kosynkin, D. V., Ceriotti, G., Wilson, K. C., Lomeda, J. R., Scorsone, J. T., Patel, A. D., Friedheim, J. E., & Tour, J. M. (2012). Graphene oxide as a high-performance fluid-loss-control additive in water-based drilling fluids. *ACS Applied Materials and Interfaces*, *4*(1), 222–227. https://doi.org/10.1021/am2012799

Mahmoud, O., Nasr-El-Din, H. A., Vryzas, Z., & Kelessidis, V. C. (2018). Effect of Ferric Oxide Nanoparticles on the Properties of Filter Cake Formed by Calcium Bentonite-Based Drilling Muds. *SPE Drilling & Completion*, *33*(04), 363–376. https://doi.org/10.2118/184572-PA

Mao, H., Qiu, Z., Shen, Z., & Huang, W. (2015). Hydrophobic associated polymer based silica nanoparticles composite with core–shell structure as a filtrate reducer for drilling fluid at utra-high temperature. *Journal of Petroleum Science and Engineering*, *129*, 1–14. https://doi.org/10.1016/J.PETROL.2015.03.003

Misbah, B., Sedaghat, A., Rashidi, M., Sabati, M., Vaidyan, K., Ali, N., Omar, M. A. A., & Hosseini Dehshiri, S. S. (2022). Friction reduction of Al2O3, SiO2, and TiO2 nanoparticles added to non-Newtonian water based mud in a rotating medium. *Journal of Petroleum Science and Engineering*, *217*, 110927. https://doi.org/10.1016/J.PETROL.2022.110927

Mohamed, A., Al-Afnan, S., Elkatatny, S., & Hussein, I. (2020). Prevention of Barite Sag in Water-Based Drilling Fluids by A Urea-Based Additive for Drilling Deep Formations. *Sustainability 2020, Vol. 12, Page 2719*, *12*(7), 2719. https://doi.org/10.3390/SU12072719

Muhsan, A. S., Mohamed, N. M., Siddiqui, U., & Shahid, M. U. (2017). Nano Additives in Water Based Drilling Fluid for Enhanced-Performance Fluid-Loss-Control. In *ICIPEG 2016*. Springer Singapore. https://doi.org/10.1007/978-981-10-3650-7_57

Nguyen, P.-T., Huu Do, B.-P., Student, S., Pham, D.-K., Nguyen, H.-A., Pham Dao, D.-Q., & Nguyen, B.-D. (2012). *Evaluation on the EOR Potential Capacity of the Synthesized Composite Silica-Core/ Polymer-Shell Nanoparticles Blended with Surfactant Systems for the HPHT Offshore Reservoir Conditions*. 12–14. http://onepetro.org/speionc/proceedings-pdf/12IONC/All-12IONC/SPE-157127-MS/1656330/spe-157127-ms.pdf/1

OFITE. (2015). *Complete HTHP Filter Press Instruction Manual*.

Okoro, E. E., Sanni, S. E., Obomanu, T., Okafor, I. S., & Emetere, M. E. (2021). Carbon Nanotubes as a Multifunctional additive and its Impact in Oil Based Mud System drilling Hydraulics. *IOP Conference Series: Earth and Environmental Science*, *665*(1). https://doi.org/10.1088/1755-1315/665/1/012004

Oseh, J. O., Mohd, N. M. N. A., Gbadamosi, A. O., Agi, A., Blkoor, S. O., Ismail, I., Igwilo, K. C., & Igbafe, A. I. (2023). Polymer nanocomposites application in drilling fluids: A review. *Geoenergy Science and Engineering*, *222*, 211416. https://doi.org/10.1016/j.geoen.2023.211416

Perumalsamy, J., Gupta, P., & Sangwai, J. S. (2021). Performance evaluation of esters and graphene nanoparticles as an additives on the rheological and lubrication properties of water-based drilling mud. *Journal of Petroleum Science and Engineering*, *204*, 108680. https://doi.org/10.1016/J.PETROL.2021.108680

Pourkhalil, H., & Nakhaee, A. (2019). Effect of Nano ZnO on wellbore stability in shale: An experimental investigation. *Journal of Petroleum Science and Engineering*, *173*, 880–888. https://doi.org/10.1016/j.petrol.2018.10.064

Ragab, A., & Noah, A. (2014). *Reduction of Formation Damage and Fluid Loss using Nano-sized Silica Drilling Fluids*.

Rana, A., Khan, I., Ali, S., Saleh, T. A., & Khan, S. A. (2020). Controlling shale swelling and fluid loss properties of water-based drilling Mud via ultrasonic impregnated SWCNTs/PVP nanocomposites. *Energy and Fuels*, *34*(8), 9515–9523. https://doi.org/10.1021/acs.energyfuels.0c01718

Razak Ismail, A., Seong, T. C., Buang, N. A., Rosli, W., & Sulaiman, W. (2014). Improve Performance of Water-based Drilling Fluids Using Nanoparticles. *Sriwijaya International Seminar on Energy and Environmental Science & Technology Palembang*.

Sadeghalvaad, M., & Sabbaghi, S. (2015). The effect of the TiO2/polyacrylamide nanocomposite on water-based drilling fluid properties. *Powder Technology*, *272*, 113–119. https://doi.org/10.1016/j.powtec.2014.11.032

Saffari, H. R. M., Soltani, R., Alaei, M., & Soleymani, M. (2018). Tribological properties of water-based drilling fluids with borate nanoparticles as lubricant additives. *Journal of*

Petroleum Science and Engineering, *171*, 253–259. https://doi.org/10.1016/J.PETROL.2018.07.049

Sajid, M., & Płotka-Wasylka, J. (2020). Nanoparticles: Synthesis, characteristics, and applications in analytical and other sciences. In *Microchemical Journal* (Vol. 154). Elsevier Inc. https://doi.org/10.1016/j.microc.2020.104623

Sajjadian, M., Sajadian, V. A., & Motlagh, E. E. (2022). Experimental analysis of improving water-based drilling fluid properties by using nanoparticles and poly (AN-co-VP)/zeolite composite. *Upstream Oil and Gas Technology*, *8*, 100066. https://doi.org/10.1016/J.UPSTRE.2022.100066

Sajjadian, M., Sajjadian, V. A., & Rashidi, A. (2020). Experimental evaluation of nanomaterials to improve drilling fluid properties of water-based muds HP/HT applications. *Journal of Petroleum Science and Engineering*, *190*. https://doi.org/10.1016/j.petrol.2020.107006

Salih, A. H., & Bilgesu, H. (2017). *Investigation of Rheological and Filtration Properties of Water-Based Drilling Fluids Using Various Anionic Nanoparticles*. http://onepetro.org/SPEWRM/proceedings-pdf/17WRM/4-17WRM/D041S015R005/1288781/spe-185638-ms.pdf/1

Sepehri, S., Soleyman, R., Varamesh, A., Valizadeh, M., & Nasiri, A. (2018). Effect of synthetic water-soluble polymers on the properties of the heavy water-based drilling fluid at high pressure-high temperature (HPHT) conditions. *Journal of Petroleum Science and Engineering*, *166*, 850–856. https://doi.org/10.1016/J.PETROL.2018.03.055

Singh, D., Singh, S., Sahu, J., Srivastava, S., & Singh, M. R. (2016). Ceramic nanoparticles: Recompense, cellular uptake and toxicity concerns. In *Artificial Cells, Nanomedicine and Biotechnology* (Vol. 44, Issue 1, pp. 401–409). Taylor and Francis Ltd. https://doi.org/10.3109/21691401.2014.955106

Singh, S., & Ahmed, R. (2010). *Vital Role of Nanopolymers in Drilling and Stimulations Fluid Applications*. 19–22. http://onepetro.org/SPEATCE/proceedings-pdf/10ATCE/All-10ATCE/SPE-130413-MS/1720046/spe-130413-ms.pdf/1

SLB. (2023a). *Fluid loss | Energy Glossary*. https://glossary.slb.com/en/terms/f/fluid_loss

SLB. (2023b). *Apparent viscosity | Energy Glossary*. https://glossary.slb.com/en/terms/a/apparent_viscosity

SLB. (2023c). *Plastic viscosity | Energy Glossary*. https://glossary.slb.com/en/terms/p/plastic_viscosity

SLB. (2023d). *Yield point | Energy Glossary*. https://glossary.slb.com/en/terms/y/yield_point

Smith, S. R., Rafati, R., Sharifi Haddad, A., Cooper, A., & Hamidi, H. (2018). Application of aluminium oxide nanoparticles to enhance rheological and filtration properties of water based muds at HPHT conditions. *Colloids and Surfaces A: Physicochemical and Engineering Aspects*, *537*, 361–371. https://doi.org/10.1016/J.COLSURFA.2017.10.050

Song, K., Wu, Q., Li, M., Ren, S., Dong, L., Zhang, X., Lei, T., & Kojima, Y. (2016). Water-based bentonite drilling fluids modified by novel biopolymer for minimizing fluid loss and formation damage. *Colloids and Surfaces A: Physicochemical and Engineering Aspects*, *507*, 58–66. https://doi.org/10.1016/J.COLSURFA.2016.07.092

Srivatsa, J. T., & Ziaja, M. B. (2012). *An Experimental Investigation on use of Nanoparticles as Fluid Loss Additives in a Surfactant-Polymer Based Drilling Fluid*. http://onepetro.org/IPTCONF/proceedings-pdf/11IPTC/All-11IPTC/IPTC-14952-MS/1668281/iptc-14952-ms.pdf/1

Sun, X., Zhang, Y., Chen, G., Gai, Z., & Wang, M. (2017). *Application of Nanoparticles in Enhanced Oil Recovery: A Critical Review of Recent Progress*. https://doi.org/10.3390/en10030345

Taha, N. M., Lee, S., & Kmc, S. (2015). *Nano Graphene Application Improving Drilling Fluids Performance*.

Van Olphen, H. (1964). Internal mutual flocculation in clay suspensions. *Journal of Colloid Science*, *19*(4), 313–322. https://doi.org/10.1016/0095-8522(64)90033-9

Vipulanandan, C., Krishnamoorti, R., Mohammed, A., Boncan, V., Narvaez, G., Hughes, B., Head, B., & Pappas, J. M. (2015). Iron Nanoparticle Modified Smart Cement for Real Time Monitoring of Ultra Deepwater Oil Well Cementing Applications. *Proceedings of the Annual Offshore Technology Conference*, *3*, 2216–2231. https://doi.org/10.4043/25842-MS

Vipulanandan, C., & Mohammed, A. (2018). *Fluid Loss Control in Smart Bentonite Drilling Mud Modified with Nanoclay and Quantified with Vipulanandan Fluid Loss Model*. http://onepetro.org/OTCONF/proceedings-pdf/18OTC/4-18OTC/D041S056R003/1194345/otc-28947-ms.pdf/1

Vipulanandan, C., Mohammed, A., & Samuel, R. G. (2017). Smart bentonite drilling muds modified with iron oxide nanoparticles & characterized based on the electrical resistivity & rheological properties with varying magnetic field strengths & temperatures. *Proceedings of the Annual Offshore Technology Conference*, *5*, 3613–3630. https://doi.org/10.4043/27626-ms

Vryzas, Z. (2016). *A Comprehensive Approach for the Development of New Magnetite Nanoparticles Giving Smart Drilling Fluids with Superior Properties for HP/HT Applications*. http://onepetro.org/IPTCONF/proceedings-pdf/16IPTC/3-16IPTC/D031S053R001/1331735/iptc-18731-ms.pdf/1

Vryzas, Z., Arkoudeas, P., Mahmoud, O., Nasr-El-Din, H., & Kelessidis, V. (2015). Utilization of Iron Oxide Nanoparticles in Drilling Fluids Improves Fluid Loss and Formation Damage Characteristics. *First EAGE Workshop on Well Injectivity and Productivity in Carbonates*, *2015*(1), 1–5. https://doi.org/10.3997/2214-4609.201412007

Vryzas, Z., Kelessidis, V. C., Nalbantian, L., Zaspalis, V., Gerogiorgis, D. I., & Wubulikasimu, Y. (2017). Effect of temperature on the rheological properties of neat aqueous Wyoming sodium bentonite dispersions. *Applied Clay Science*, *136*, 26–36. https://doi.org/10.1016/j.clay.2016.11.007

Vryzas, Z., Zaspalis, V., Nalbandian, L., Terzidou, A., & Kelessidis, V. C. (2018). Rheological and HP/HT fluid loss behavior of nano-based drilling fluids utilizing Fe 3 O 4 nanoparticles. In *Materials Today: Proceedings* (Vol. 5). www.sciencedirect.comwww.materialstoday.com/proceedings2214-7853

Vryzas, Z., Zaspalis, V., Nalbantian, L., Mahmoud, O., Nasr-El-Din, H. A., & Kelessidis, V. C. (2016). *A Comprehensive Approach for the Development of New Magnetite Nanoparticles Giving Smart Drilling Fluids with Superior Properties for HP/HT Applications*. https://doi.org/10.2523/IPTC-18731-MS

Wang, Z., Xu, Y., Gan, Y., Han, X., Liu, W., & Xin, H. (2022). Micromechanism of partially hydrolyzed polyacrylamide molecule agglomeration morphology and its impact on the stability of crude oil−water interfacial film. *Journal of Petroleum Science and Engineering*, *214*, 110492. https://doi.org/10.1016/J.PETROL.2022.110492

Xie, B., & Liu, X. (2017). Thermo-thickening behavior of LCST-based copolymer viscosifier for water-based drilling fluids. *Journal of Petroleum Science and Engineering*, *154*, 244–251. https://doi.org/10.1016/J.PETROL.2017.04.037

Xionghu, Z., Egwu, S. B., Jingen, D., Liujie, M., & Xiangru, J. (2022). Synthesis of Asphalt Nanoparticles and Their Effects on Drilling Fluid Properties and Shale Dispersion. *SPE Drilling and Completion*, *37*(1), 67–76. https://doi.org/10.2118/208589-PA

Xuan, Y., Jiang, G., & Li, Y. (2014). Nanographite Oxide as Ultrastrong Fluid-Loss-Control Additive in Water-Based Drilling Fluids. *Http://Dx.Doi.Org/10.1080/01932691.2013.858350*, *35*(10), 1386–1392. https://doi.org/10.1080/01932691.2013.858350

Yang, P., Li, T. B., Wu, M. H., Zhu, X. W., & Sun, X. Q. (2015). Analysis of the effect of polyanionic cellulose on viscosity and filtrate volume in drilling fluid. *Https://Doi.Org/10.1179/1432891715Z.0000000001329*, *19*, S512–S516. https://doi.org/10.1179/1432891715Z.0000000001329

Yang, X., Shang, Z., Liu, H., Cai, J., & Jiang, G. (2017). Environmental-friendly salt water mud with nano-SiO2 in horizontal drilling for shale gas. *Journal of Petroleum Science and Engineering*, *156*, 408–418. https://doi.org/10.1016/J.PETROL.2017.06.022

Zhao, X. H., Li, W., Li, S. L., & Ji, Y. H. (2013). Application of several kinds of clays and a new type of nano-modified bontonite in drilling fluids. *Advanced Materials Research*, *746*, 489–495. https://doi.org/10.4028/www.scientific.net/AMR.746.489

Zhong, H., Guan, Y., Qiu, Z., Feng, J., Liu, W., Wan, Y., & Zhang, Y. (2021). Improvement of Rheological and Filtration Properties of Water-Based Drilling Fluids Using Bentonite-Hydrothermal Carbon Nanocomposites Under the Ultra-High Temperature and High Pressure Conditions. *Society of Petroleum Engineers - SPE/IATMI Asia Pacific Oil and Gas Conference and Exhibition 2021, APOG 2021*, 12–14. https://doi.org/10.2118/205539-MS

Zhong, H., Shen, G., Qiu, Z., Lin, Y., Fan, L., Xing, X., & Li, J. (2019). Minimizing the HTHP filtration loss of oil-based drilling fluid with swellable polymer microspheres. *Journal of Petroleum Science and Engineering*, *172*, 411–424. https://doi.org/10.1016/J.PETROL.2018.09.074

Zhong, H., Yang, T., Yin, H., Lu, J., Zhang, K., & Fu, C. (2020). Role of Alkali Type in Chemical Loss and ASP-Flooding Enhanced Oil Recovery in Sandstone Formations. *SPE Reservoir Evaluation & Engineering*, *23*(02), 431–445. https://doi.org/10.2118/191545-PA